CVR-2022-0689

# Supplementary material

## Phospholamban pentamerization increases sensitivity and dynamic range of cardiac relaxation

Short title: PLN pentamers extend the regulation of cardiac function

Florian Funk, PhD[1], Annette Kronenbitter, PhD[1], Katarzyna Hackert, PhD[1], Matthias Oebbeke[2], M.Sc., Gerhard Klebe, PhD[2], Mareike Barth, PhD[3], Daniel Koch, MD, PhD[4], Joachim P. Schmitt, MD[1]*

[1]Institute of Pharmacology, University Hospital Düsseldorf, and Cardiovascular Research Institute Düsseldorf (CARID), Heinrich-Heine-University, Universitätsstraße 1, 40225 Düsseldorf, Germany; [2]Institute of Pharmaceutical Chemistry, Philipps-University Marburg, Marbacher Weg 6, 35032 Marburg, Germany; [3]Department of Cardiovascular Surgery, University Hospital Düsseldorf, Heinrich-Heine-University, Moorenstr. 5, 40225 Düsseldorf, Germany; [4]Max Planck Institute for Neurobiology of Behavior - caesar, Ludwig-Erhard-Allee 2, 53175 Bonn, Germany

*Correspondence to:
Joachim P. Schmitt, MD
Institute of Pharmacology and Clinical Pharmacology,
University Hospital Düsseldorf
Universitätsstraße 1, 40225 Düsseldorf, Germany
phone: +49-211-8112449
fax: +49-211-8114781
email: joachim.schmitt@uni-duesseldorf.de

## Expanded Materials and Methods

**Fluorescence staining of isolated cardiomyocytes.** Myocytes were isolated by digestion of mouse hearts with collagenase type I as described above and spread on laminin-coated coverslips before fixing in 4 % paraformaldehyde. Cells were washed in PBS, permeabilized with 0.1 % Triton™ X-100 for 5 min, washed again and incubated in 0.05 % Tween 20 plus 1 % BSA and the primary antibody in a 1:50 dilution for 1 h (anti-FLAG, (clone M2, Sigma), anti-SERCA2a (A010-20, Badrilla), anti-MyBP-C3 (M-190, Santa Cruz). After washing with 0.1 % Tween 20, cells were incubated with secondary antibodies for 1 h (goat anti-mouse Alexa Fluor®488 conjugate and goat anti-rabbit Alexa Fluor®546 conjugate, Thermo Fisher Scientific). Staining was visualized at 488 nm and 546 nm, respectively, using a confocal Laser Scanning Microscope (LSM 700, Zeiss).

## Expanded Results

**PLN expression patterns and basal characterization of mouse models TgPLN and TgAFA-PLN.** Mice expressing PLN, respectively AFA-PLN, transgenes in a PLN-deficient genetic background were designated as TgPLN and TgAFA-PLN. Total PLN expression was about 20 % higher in heart tissue of TgPLN compared to the purely monomeric TgAFA-PLN (Fig. S3C), however the proportion of PLN monomers, representing the PLN species known to inhibit SERCA2a, was 2.2-fold higher in TgAFA-PLN hearts on SDS gel (Fig. S3D). Importantly, PLN expression and the pentamer/monomer distribution of TgPLN mice were similar to endogenous PLN of age- and strain-matched wild-type mice (Fig. S3D). Cardiac gross morphology and histology of TgPLN, TgAFA-PLN, PLN-KO and wild-type mice were indistinguishable. Transgenic mice showed regular heart size, shape and myocardial texture at the age of 20 weeks (Fig. S5A). There was no evidence of increased interstitial collagen and echocardiographic analyses demonstrated age-appropriate wall thickness, left ventricular dimensions and contraction both in young adults (8 weeks old) and aging TgPLN, TgAFA-PLN and PLN-KO mice (8 months old) (Table S2, S3). Importantly, heart size and function of TgPLN was also indistinguishable from age- and strain-matched wild-type animals (Table S1).

The same way as TgPLN and TgAFA-PLN mice, we generated two additional transgenic mouse lines that expressed PLN, respectively AFA-PLN, fused to an N-terminal FLAG epitope, designated TgF-PLN and TgF-AFA-PLN. These mice also developed normally, lived longer than one year and expressed the transgenes at comparable levels (threshold cycle at qPCR 12.0 ± 0.2 versus 12.4 ± 0.4, $N$ = 3 per group). TgF-PLN and TgF-AFA-PLN mice were used for subcellular localization of PLN and AFA-PLN in isolated cardiomyocytes by anti-FLAG-antibodies to rule out ectopic localization of transgene encoded proteins. Immunofluorescence staining demonstrated an orderly pattern of cross striations both for F-PLN and F-AFA-PLN that co-localized with SERCA2a (Fig. S5). Counterstaining with antibodies against myosin binding protein C (MyBP-C) confirmed the localization of the SR membrane proteins PLN and SERCA2a outside the sarcomeres of cardiomyocytes. Mouse lines TgF-PLN and TgF-AFA-PLN were further used for western blot analyses to detect PLN and AFA-PLN transgenes independent of anti-PLN antibodies (Fig. 2D).

CVR-2022-0689

## Supplementary Figure S1

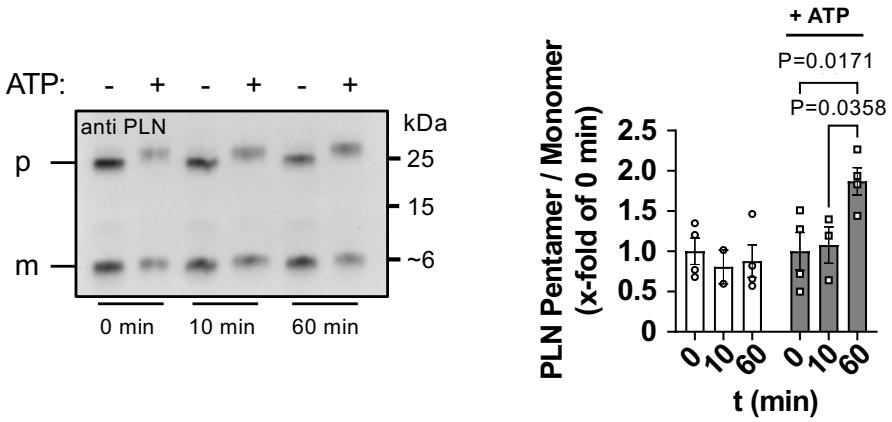


**Figure S1. Dynamics of PLN pentamerization in dependence on the phosphorylation status.** Synthetic PLN was PKA-phosphorylated for 30 minutes (25 U/µL PKA) at 30 °C. Control samples (white bars) were treated identically but without ATP addition. Reactions were stopped by addition of SDS-PAGE sample buffer and samples were further incubated for 0, 10 and 60 minutes. Ratios of PLN pentamers and monomers were analyzed by western blotting. An increase in the ratio of pentamers/monomers was apparent only in the phosphorylated samples after 60, but not 10 minutes. Groups were analyzed by Mixed-effects model (REML) followed by Tukey's multiple comparisons test; N=2-4.

## Supplementary Figure S2

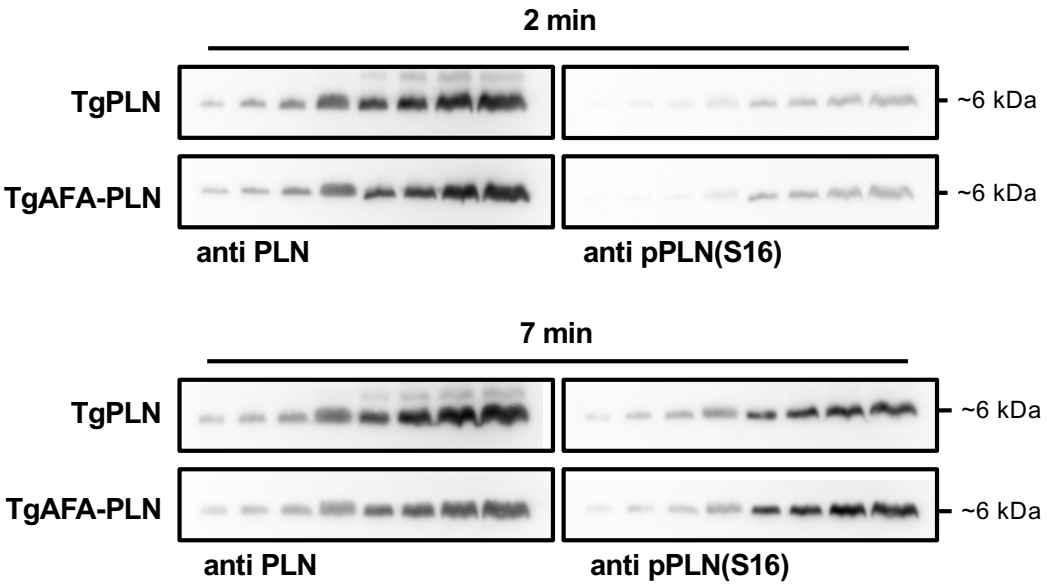


**Figure S2. Kinetics of PKA-dependent phosphorylation of PLN and AFA-PLN monomers.** Different amounts (0.3, 0.6, 1, 3, 6, 10, 20, 30 µg) of dephosphorylated homogenates of TgPLN and TgAFA-PLN were boiled and blotted to PVDF membrane to avoid presence of PLN pentamers during the following phosphorylation reaction with PKA (0.5 U / µL) for 2 and 7 minutes. PKA-dependent phosphorylation at S16 was analyzed using phospho-specific antibodies (anti pPLN(S16)).

## Supplementary Figure S3

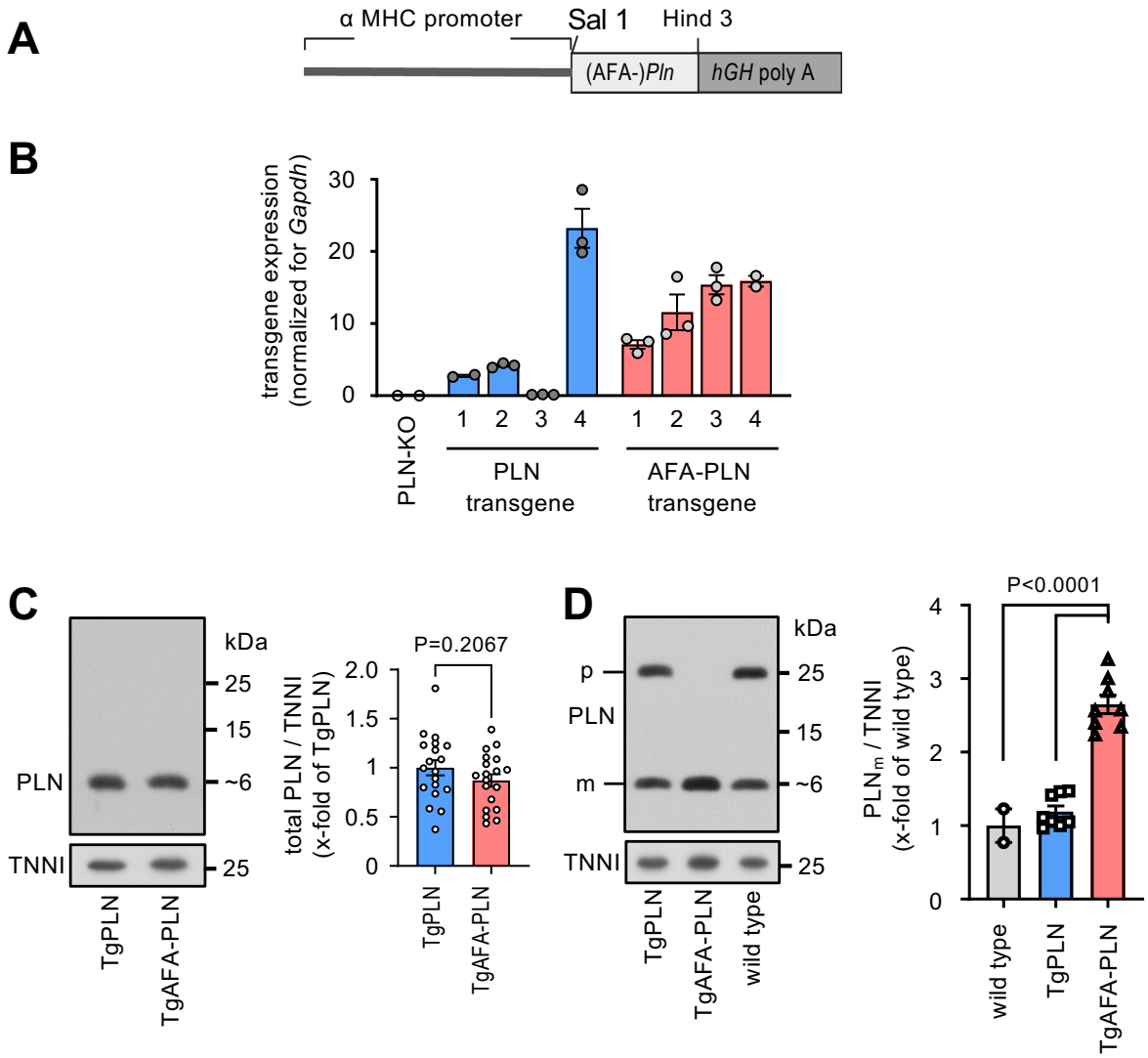


**Figure S3. Generation of transgenic mice that express either wild type PLN or only monomeric PLN.** (A) Schematic representation of the genetic constructs for oocyte injection; cDNA of PLN (wild-type PLN expressing monomers and pentamers) or AFA-PLN (expressing only monomers) was cloned downstream of the murine α-myosin heavy chain (α-MHC) promoter. hGH, human growth hormone polyadenylation signal; restriction sites used for cloning are indicated; (B) relative mRNA levels of cardiac transgenes assessed by qPCR for 4 founder lines per genotype. *N* = 3 hearts per mouse line. Owing to their similar levels of transgene expression mouse lines #2 (PLN transgene) and #1 (AFA-PLN transgene) were deleted from endogenous PLN by cross-breeding with PLN-deficient mice and designated as TgPLN and TgAFA-PLN. (C) Protein expression levels of total PLN determined by western blotting of TgPLN and TgAFA-PLN heart lysates and anti-PLN antibodies. Samples were heated to 95 °C for 5 min to dissolve PLN pentamers; *N* = 8 hearts per group. *P* value by Student's *t* test. (D) Expression levels of PLN monomers (m) and pentamers (p) in TgPLN, TgAFA-PLN and wild type hearts; right, quantitative analysis of monomeric bands; TgPLN, *N* = 8 hearts; TgAFA-PLN, *N* = 8 hearts; wild type, *N* = 2 hearts; equal amounts of total protein were loaded in all lanes shown in (C) and (D), cardiac troponin I (TNNI) served as loading control; *P* values by one-way ANOVA followed by Tukey's multiple comparisons test.

## Supplementary Figure S4

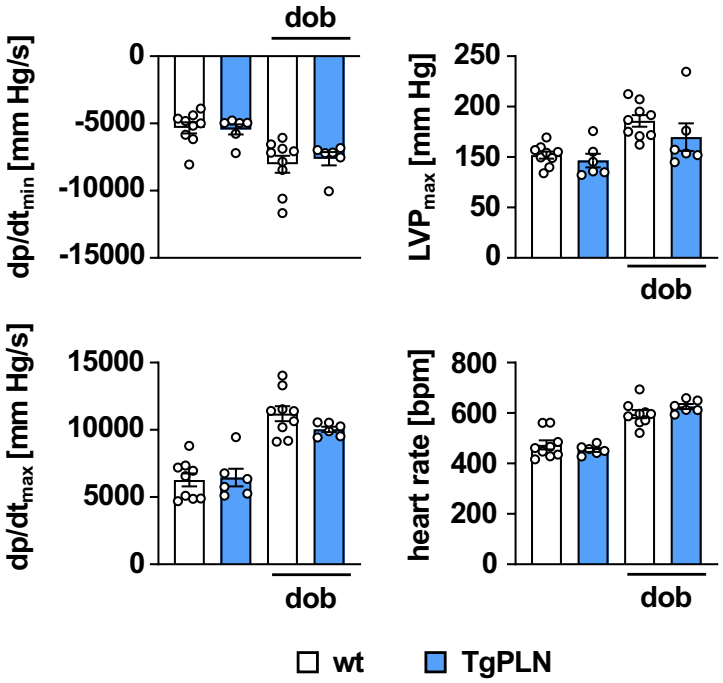


**Figure S4. Left ventricular hemodynamics of TgPLN are indistinguishable from wild-type mice.** Speed of LV pressure decay ($dp/dt_{min}$) and pressure rise ($dp/dt_{max}$), maximum pressure ($LVP_{max}$) and heart rate were determined by LV catheterization of anesthetized mice at the age of 8-10 weeks. Measurements were obtained before and after intravenous infusion of 1.5 µg/min dobutamine (dob).

## Supplementary Figure S5

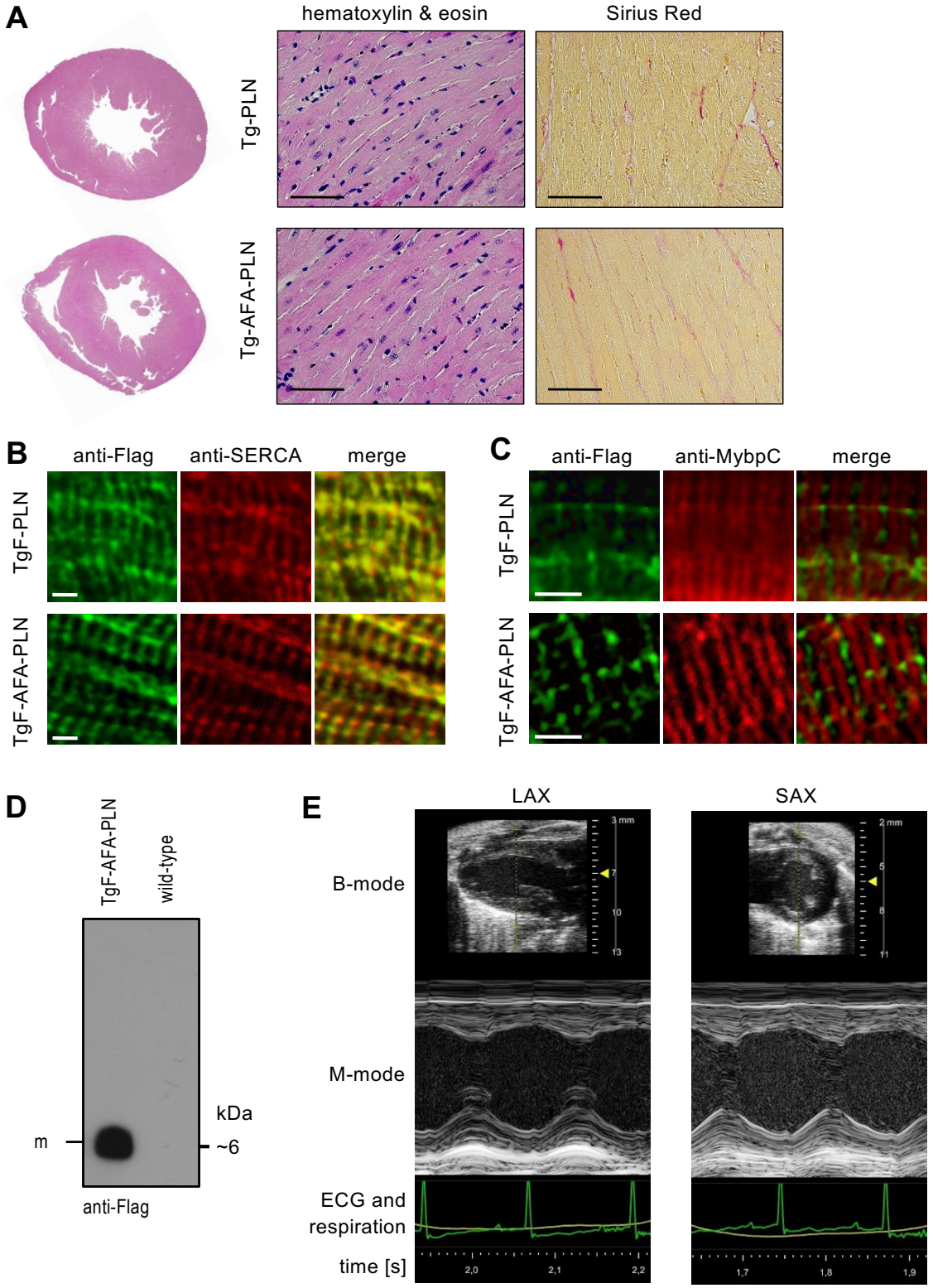


**Figure S5. Characterization of TgPLN and TgAFA-PLN mouse hearts.** (A) Regular gross morphology of TgPLN and TgAFA-PLN mouse hearts. Transverse mid-ventricular sections and histological sections stained with hematoxylin and eosin or Sirius Red of 20 week-old hearts; scale bars, 50 µm; (B) PLN and AFA-PLN (green) co-localize with SERCA2a (red) in cardiomyocytes from transgenic mice expressing N-terminally FLAG-tagged PLN (TgF-PLN) or AFA-PLN (TgF-AFA-PLN), respectively; scale bars, 2.5 µm; (C) PLN and AFA-PLN (green) do not co-localize with the sarcomeric protein myosin binding protein C (MybpC; red); scale bars, 2.5 µm. Staining of wild-type mice with anti-Flag antibodies yielded no signal (data not shown). (D) The specificity of anti-Flag antibodies was further validated by western blotting. (E) Representative echocardiographic recordings. LAX, long axis view, SAX, short axis view.

## Supplementary Figure S6

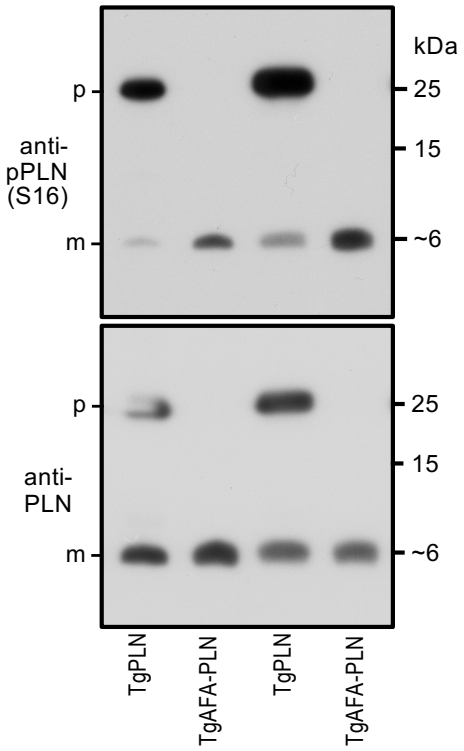


**Figure S6. PLN monomer phosphorylation is reduced in the presence of pentamers.** Western blot using heart lysates of TgPLN and TgAFA-PLN (2 representative mice per mouse line) and antibodies against PLN phosphorylated at S16 (anti-pPLN(S16)) and total PLN (anti-PLN); mice were under resting conditions (without anesthesia) at the time of cervical dislocation and organ harvest. m, monomers; p, pentamers.

## Supplementary Figure S7

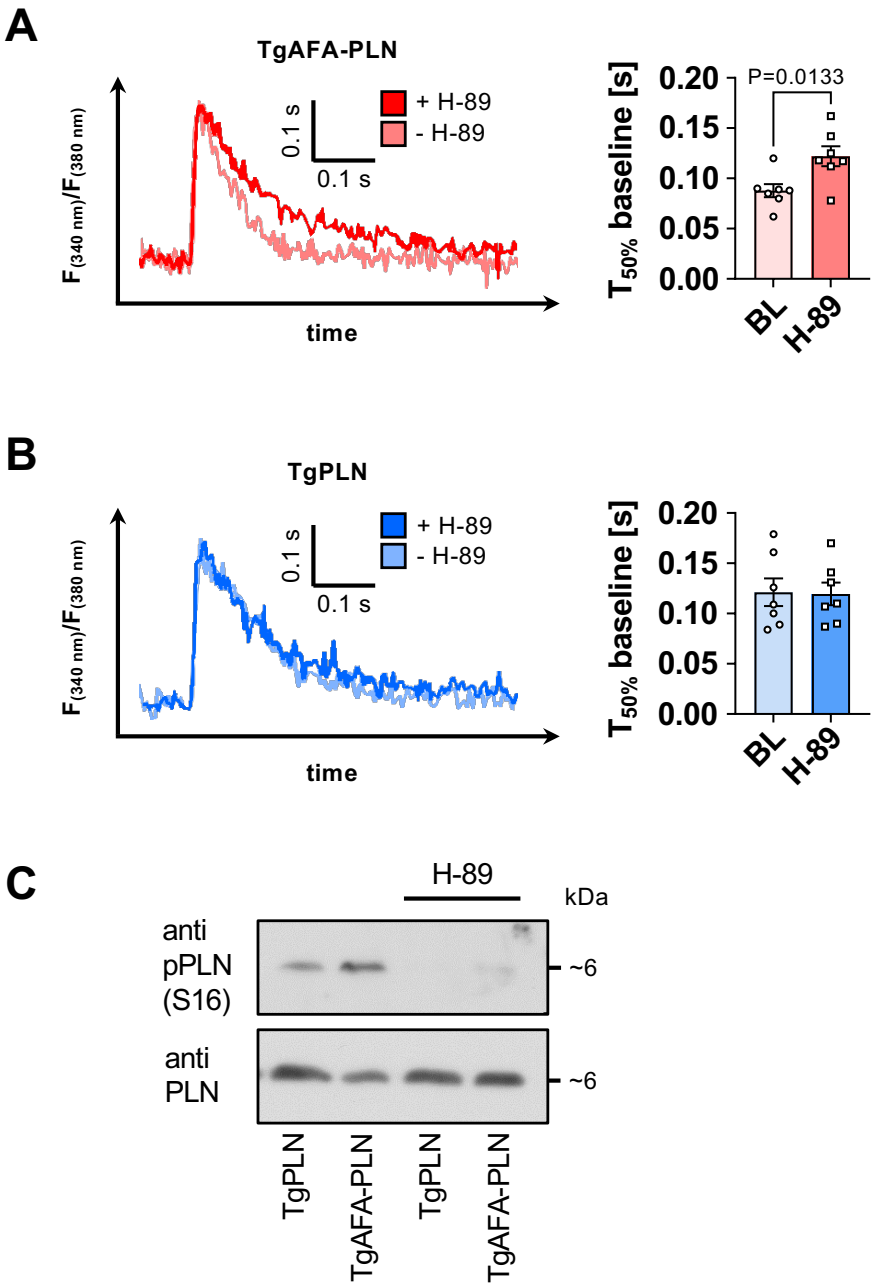


**Figure S7. Cardiomyocyte SR $Ca^{2+}$ uptake rates of TgPLN and TgAFA-PLN cardiomyocytes are comparable in the absence of PKA-dependent PLN phosphorylation.** Measurements of $Ca^{2+}$ transients in isolated and electrically paced cardiomyocytes (0.5 Hz) of TgPLN and TgAFA-PLN mice. Representative recordings (left) and duration of cytosolic $Ca^{2+}$ elimination of TgAFA-PLN (A) and TgPLN (B) at baseline and during treatment with PKA-inhibitor (H-89, $10^{-5}$ M). N = 7 hearts and 70 – 77 cells per group; comparison of groups by unpaired two-tailed Student's *t* test, *P <0.05. (C) Immunoblot using isolated myocytes from TgPLN and TgAFA-PLN hearts and antibodies against phosphorylated S16 (anti-pPLN(S16)) and total PLN (anti-PLN). Left, phosphorylation patterns of PLN monomers at baseline; right, phosphorylation patterns after 15 min incubation with the PKA inhibitor H-89 ($10^{-5}$ M) at 37 °C.

## Supplementary Figure S8

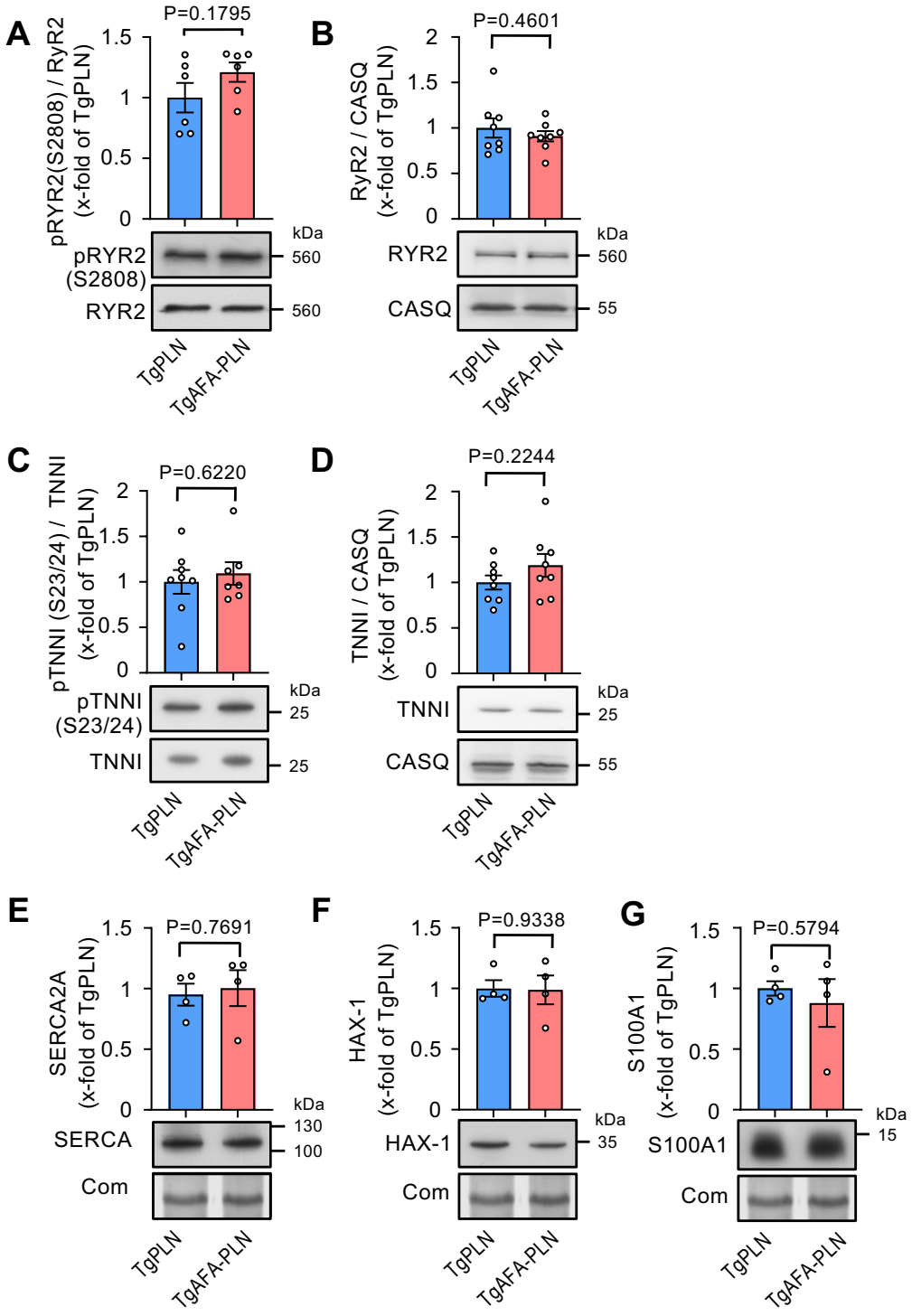


**Figure S8. Expression and PKA-dependent phosphorylation of $Ca^{2+}$ regulators other than pPLN(S16) are unchanged.** (A-E) Representative immunoblots using TgPLN and TgAFA-PLN heart lysates and antibodies against (A) PKA-dependent phosphorylated cardiac ryanodine receptor (pRyR2) and (B) total RyR2, (C) PKA-dependent phosphorylated cardiac troponin I (pTNNI) and (D) total troponin I (TNNI), (E) SERCA2A, (F) HAX-1 and (G) S100A1 expression; *N* = 4 to 8 hearts per group; Coomassie staining of gels (Com) confirmed equal loading. *P* values by Student's *t* test.

## Supplementary Figure S9

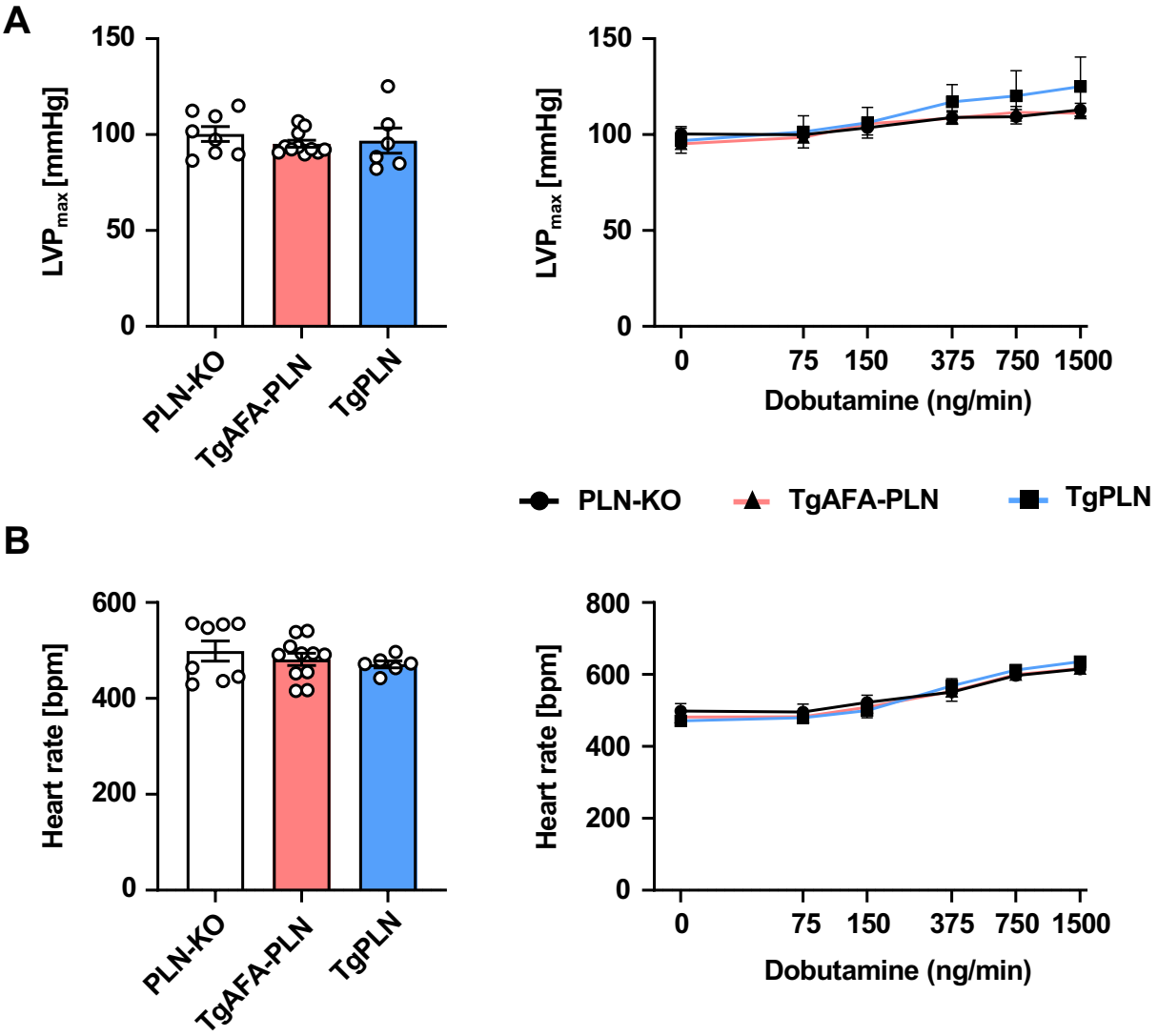


**Figure S9. Invasive measurements of maximal left ventricular pressure (LVPmax) and heart rate.** 8-week-old TgPLN, TgAFA-PLN and PLN-KO mice were subjected to left ventricular catheterization via the right carotid artery under baseline conditions (left) and during intravenous application of dobutamine at increasing concentrations (right); N = 6 animals per group.

## Supplementary Figure S10

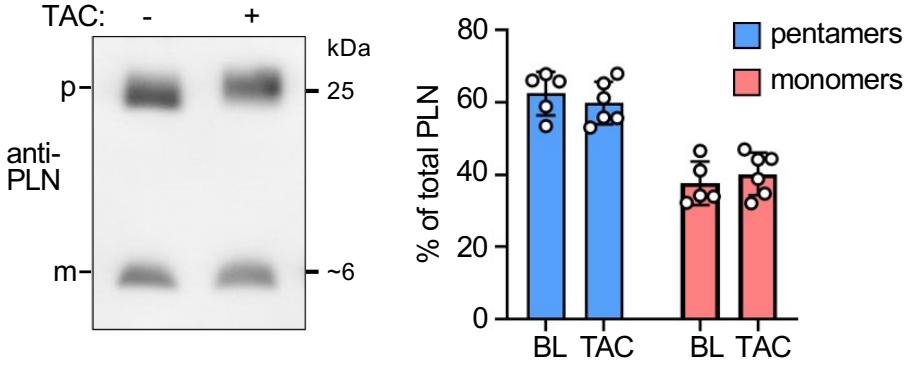


**Figure S10. Left ventricular pressure overload does not affect the pentamer-to-monomer ratios of PLN.** Western blot analysis for PLN pentamers and monomers using left ventricular heart tissue of TgPLN mice without (baseline; BL) and one week after TAC surgery (TAC). p, PLN pentamers; m. PLN monomers; mean ± SEM, n = 5-6 hearts.

## Supplementary Figure S11

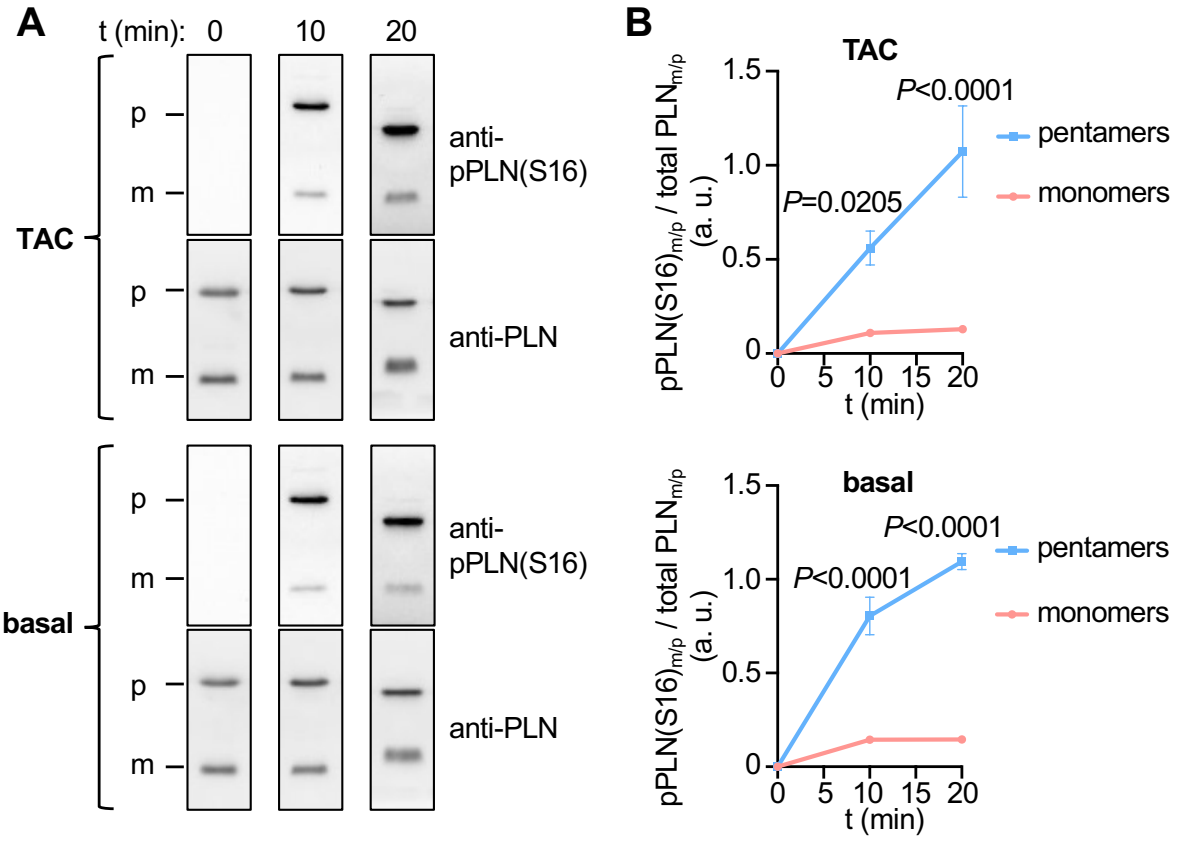


**Figure S11. Left ventricular pressure overload does not affect the phosphorylation rates of PLN pentamers and monomers.** (A) Far western kinase assay using TgPLN left ventricular (LV) heart tissue without (basal) and one week after transverse aortic constriction (TAC) as detailed in methods section. LV lysates were dephosphorylated and monomers and pentamers were separated and fixed to PVDF membrane prior to phosphorylation with PKA for 0, 10 and 20 min and Western blot analysis using antibodies against S16-phosphorylated (anti-pPLN(S16)) and total PLN (anti-PLN). (B) Signal intensities of PKA-dependent monomer (pentamer) phosphorylation at S16 normalized to total PLN monomer (pentamer) signals; p, PLN pentamers (25 kDa); m, PLN monomers (~6 kDa); a. u., arbitrary units; *P* values by two-way ANOVA and mixed-effects model (REML) followed by Sidak's multiple comparisons test; mean ± SEM, n = 4-6 hearts (TAC) and n = 3 hearts (basal).

## Supplementary Figure S12

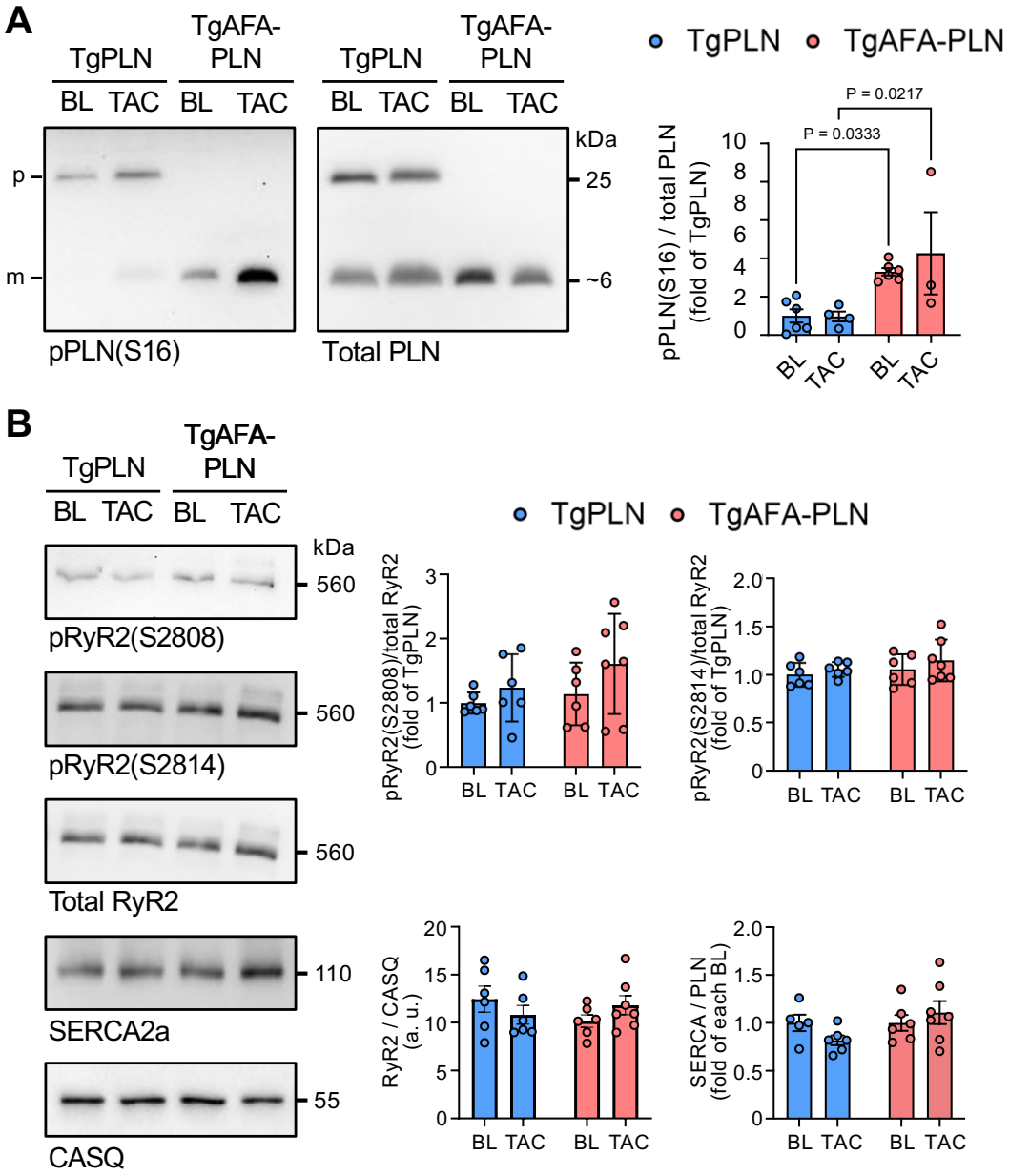


**Figure S12. Phosphorylation and/or expression of PLN, RyR2 and SERCA2a in pressure-overloaded hearts.** Western blot analysis of left ventricular heart tissue from TgPLN and TgAFA-PLN at baseline (BL) and one week after transverse aortic constriction surgery (TAC).; (A) PLN, phospholamban; pPLN(S16), phospholamban phosphorylated at S16; p / m PLN pentamers / monomers; RyR2, ryanodine receptor 2; pRyR2, RyR2 phosphorylated at indicated phosphorylation site; SERCA2a, sarco-/endoplasmic reticulum $Ca^{2+}$-ATPase; CASQ, calsequestrin; *P* values by one-way ANOVA followed by Sidak's multiple comparisons test; mean ± SEM, n = 6-7.

## Supplementary Figure S13

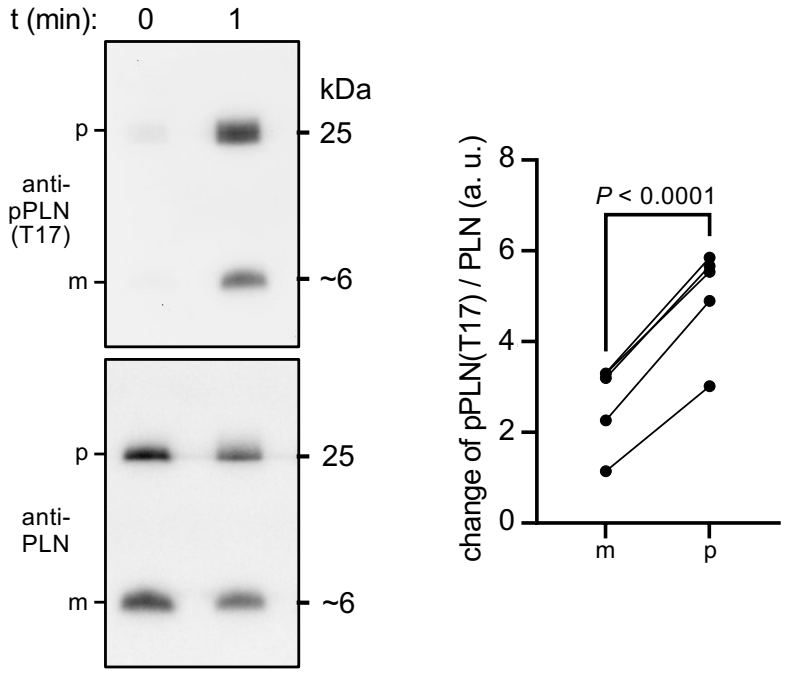


**Figure S13. Phosphorylation of PLN monomers and pentamers at T17 upon CamKII stimulation.** (A) Western blot analysis of PLN monomer (m) and pentamer (p) T17 phosphorylation (anti-pPLN-T17 antibodies, Badrilla, Cat. # A010-13) compared to total PLN in the respective fraction. Isolated adult mouse cardiomyocytes were analyzed without (t=0 min) or after 1 min exposure to 1 mM $Ca^{2+}$ that would activate $Ca^{2+}$/calmodulin-dependent kinase (CamK) II. (B) Change of pentamer and monomer T17 phosphorylation within 1 min of exposure to 1 mM $Ca^{2+}$ (n = 5 hearts). Note the faster increase of pentamer phosphorylation at T17 compared to monomers. *P* value by paired *t* test.

## Supplementary Figure S14

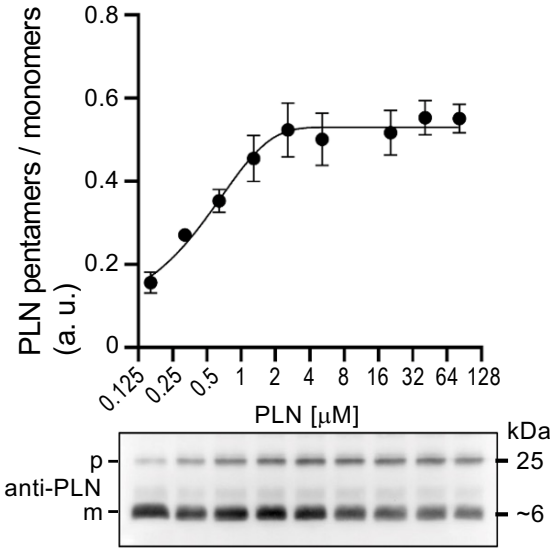


**Figure S14. PLN pentamer-to-monomer ratios depend on the concentration of PLN.** Synthetic PLN was solubilized (see methods) at the indicated concentrations and incubated at room temperature for 2 hours. Equal amounts of PLN were analyzed by Western blotting and signals of monomers and pentamers were quantified. n = 3-4 technical replicates.

## Supplementary Figure S15

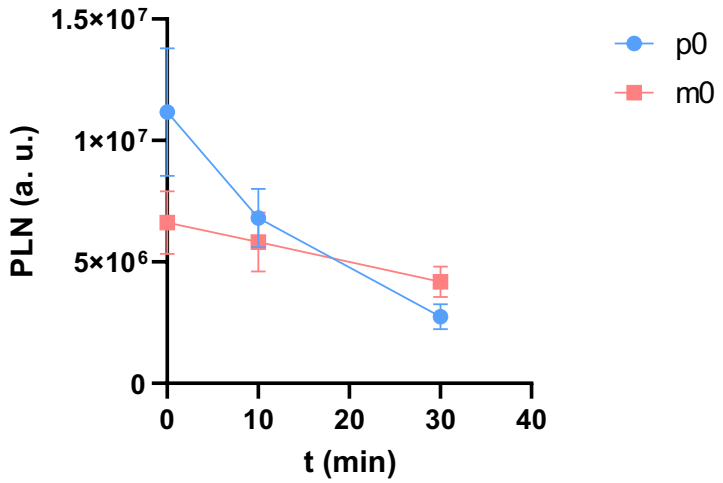


**Figure S15. Time course of PKA-dependent phosphorylation of PLN monomers and pentamers.** Synthetic PLN was phosphorylated by PKA for 0, 10 and 30 min in solution followed by western blot using Phos-tag™-gels and anti-PLN antibodies (as shown in Fig. 1D of the main manuscript). Chemiluminescent signals of unphosphorylated pentameric ($p_0$) and unphosphorylated monomeric bands ($m_0$) were visualized using a CCD camera system and quantified by ChemStudio software (VisionWorks, AnalytikJena). The graph shows the raw data at the different time points after starting the phosphorylation reaction. Note the steeper decline of $p_0$ compared to $m_0$ indicating faster depletion of unphosphorylated PLN pentamers. Mean ± SEM, N=6 independent experiments.

## Supplementary Figure S16

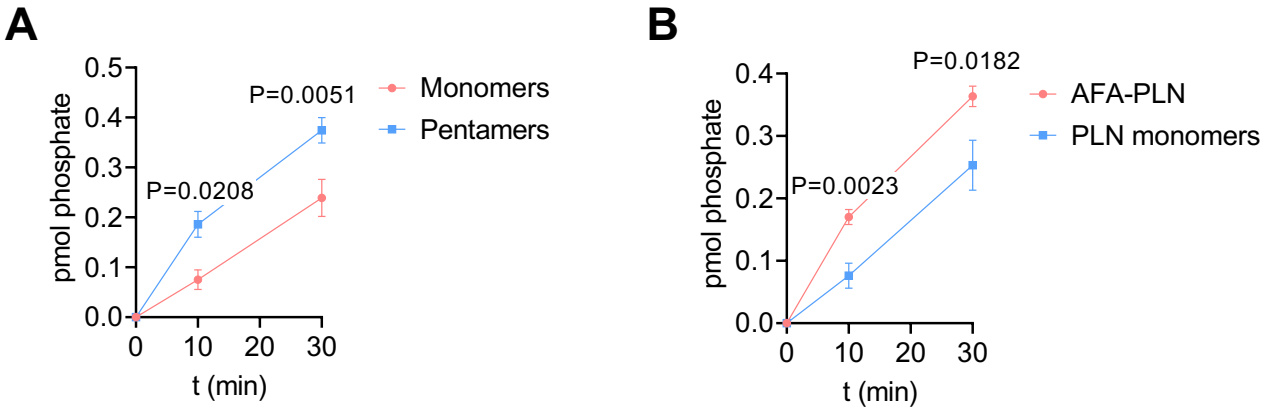


**Fig. S16. PLN pentamers are excellent PKA substrates.** (A) *In vitro* phosphorylation of synthetic PLN (adjusted for equal monomer amounts) by PKA for 0, 10 and 30 min in solution followed by western blot using Phos-tag™-gels and anti-PLN antibodies. The amount of phosphate incorporation (pmol) was calculated from quantification of figure 1D by considering the total amount of synthetic PLN loaded to the gels. Signals of pentameric phospho-species ($p_1$, $p_2$, $p_3$) were adjusted for the respective phosphate content (i. e. $p_1 \times 0.2$, $p_2 \times 0.4$, $p_3 \times 0.6$). (B) Quantification of phosphate incorporation into AFA-PLN and PLN monomers as in (A). Mean ± SEM, N=6, P values by two-way ANOVA followed by Sidak's multiple comparisons test.

## Supplementary Table S1

**Table S1. Echocardiography of 8-10 week-old wild-type and TgPLN mice**

| | wt | TgPLN | *P* |
|---|---|---|---|
| **N** | 7 | 8 | |
| **LVAW;d [mm]** | 0.72 ± 0.05 | 0.72 ± 0.04 | 0.99 |
| **LVPW;d [mm]** | 0.75 ± 0.05 | 0.69 ± 0.04 | 0.35 |
| **LVID;d [mm]** | 3.13 ± 0.12 | 3.05 ± 0.13 | 0.67 |
| **LVID;s [mm]** | 1.96 ± 0.05 | 2.06 ± 0.13 | 0.51 |
| **FS [%]** | 37 ± 2 | 33 ± 2 | 0.19 |
| **LV volume;d [µl]** | 30 ± 3 | 28 ± 3 | 0.58 |
| **LV volume;s [µl]** | 10 ± 1 | 11 ± 2 | 0.62 |
| **LV mass [mg]** | 72 ± 7 | 65 ± 5 | 0.37 |
| **heart rate [bpm]** | 507 ± 27 | 486 ± 11 | 0.47 |

N, number of mice studied; LVAW, left ventricular anterior wall thickness; d, diastolic; LVPW, left ventricular posterior wall thickness; LVID, left ventricular internal dimension; s, systolic; FS, fractional shortening; bpm, beats per min. *P* values by unpaired Student's *t* test.

## Supplementary Table S2

**Table S2: Echocardiography of 8-weeks-old mice**

| | PLN-KO | TgAFA-PLN | *P* vs. PLN-KO | TgPLN | *P* vs. PLN-KO | *P* vs. TgAFA-PLN |
|---|---|---|---|---|---|---|
| **N** | 8 | 8 | | 8 | | |
| **LVAW;d [mm]** | 0.74 ± 0.04 | 0.72 ± 0.04 | 0.94 | 0.72 ± 0.04 | 0.92 | 0.99 |
| **LVPW;d [mm]** | 0.74 ± 0.02 | 0.66 ± 0.02 | 0.22 | 0.69 ± 0.04 | 0.44 | 0.87 |
| **LVID;d [mm]** | 3.07 ± 0.13 | 2.98 ± 0.11 | 0.87 | 3.05 ± 0.13 | 0.99 | 0.93 |
| **LVID;s [mm]** | 1.99 ± 0.14 | 1.97 ± 0.15 | 0.99 | 2.06 ± 0.13 | 0.94 | 0.89 |
| **FS [%]** | 35 ± 2 | 35 ± 3 | 0.98 | 33 ± 2 | 0.77 | 0.87 |
| **LV volume;d [µl]** | 29 ± 3 | 26 ± 3 | 0.76 | 28 ± 3 | 0.94 | 0.93 |
| **LV volume;s [µl]** | 11 ± 2 | 10 ± 2 | 0.97 | 11 ± 2 | 0.99 | 0.95 |
| **heart rate [bpm]** | 504 ± 6 | 474 ± 17 | 0.17 | 486 ± 11 | 0.47 | 0.72 |

N, number of mice studied; LVAW, left ventricular anterior wall thickness; d, diastolic; LVPW, left ventricular posterior wall thickness; LVID, left ventricular internal dimension; s, systolic; FS, fractional shortening; bpm, beats per min. *P* values by one-way ANOVA followed by Tukey's multiple comparisons test.

## Supplementary Table S3

**Table S3: Echocardiography of 8-months-old mice**

| | PLN-KO | TgAFA-PLN | *P* vs. PLN-KO | TgPLN | *P* vs. PLN-KO | *P* vs. TgAFA-PLN |
|---|---|---|---|---|---|---|
| **N** | 6 | 6 | | 6 | | |
| **LVAW;d [mm]** | 0.93 ± 0.04 | 0.91 ± 0.04 | 0.94 | 1.00 ± 0.04 | 0.40 | 0.24 |
| **LVPW;d [mm]** | 0.85 ± 0.01 | 0.84 ± 0.04 | 0.96 | 0.93 ± 0.04 | 0.21 | 0.13 |
| **LVID;d [mm]** | 3.67 ± 0.17 | 3.63 ± 0.16 | 0.98 | 3.58 ± 0.22 | 0.94 | 0.98 |
| **LVID;s [mm]** | 2.14 ± 0.14 | 1.99 ± 0.13 | 0.86 | 2.16 ± 0.30 | 0.99 | 0.83 |
| **FS [%]** | 42 ± 1 | 45 ± 2 | 0.73 | 41 ± 4 | 0.98 | 0.63 |
| **LV volume;d [µl]** | 58 ± 17 | 57 ± 15 | 0.99 | 55 ± 9 | 0.97 | 0.99 |
| **LV volume;s [µl]** | 16 ± 3 | 14 ± 2 | 0.94 | 19 ± 6 | 0.90 | 0.73 |
| **heart rate [bpm]** | 531 ± 40 | 558 ± 20 | 0.75 | 567 ± 19 | 0.64 | 0.97 |

N, number of mice studied; LVAW, left ventricular anterior wall thickness; d, diastolic; LVPW, left ventricular posterior wall thickness; LVID, left ventricular internal dimension; s, systolic; FS, fractional shortening; bpm, beats per min. *P* values by one-way ANOVA followed by Tukey's multiple comparisons test.

## Supplementary Table S4

**Table S4: $Ca^{2+}$ kinetics in isolated myocytes.**

| **baseline traces** | PLN-KO | TgAFA-PLN | *P* vs. PLN-KO | TgPLN | *P* vs. PLN-KO | *P* vs. TgAFA-PLN |
|---|---|---|---|---|---|---|
| **N** | 8 | 8 | | 8 | | |
| **amplitude [ΔF]** | 0.58 ± 0.05 | 0.59 ± 0.05 | 0.99 | 0.51 ± 0.05 | 0.61 | 0.54 |
| **vel increase [ΔF $s^{-1}$]** | 36 ± 4 | 41 ± 3 | 0.66 | 34 ± 4 | 0.91 | 0.41 |
| **vel decrease [ΔF $s^{-1}$]** | 3.9 ± 0.5 | 3.5 ± 0.5 | 0.82 | 2.1 ± 0.2 | **0.03** | 0.10 |

| **$10^{-7}$ M isoproterenol** | PLN-KO | TgAFA-PLN | P vs. PLN-KO | TgPLN | P vs. PLN-KO | P vs. TgAFA-PLN |
|---|---|---|---|---|---|---|
| **N** | 11 | 11 | | 11 | | |
| **amplitude [ΔF]** | 0.94 ± 0.08 | 0.99 ± 0.08 | 0.91 | 0.97 ± 0.06 | 0.97 | 0.98 |
| **vel increase [ΔF $s^{-1}$]** | 68 ± 6 | 78 ± 8 | 0.58 | 78 ± 6 | 0.60 | 0.99 |
| **vel decrease [ΔF $s^{-1}$]** | 6.9 ± 0.8 | 6.9 ± 0.8 | 0.99 | 6.0 ± 0.5 | 0.64 | 0.64 |

N, number of hearts; amplitude, peak height of the $Ca^{2+}$ transient; ΔF, change of fluorescence (340/380nm); vel increase (decrease), velocity of transient increase (decrease); *P* values by one-way ANOVA followed by Tukey's multiple comparisons test.

## Supplementary Table S5

**Table S5: $Ca^{2+}$ kinetics in isolated myocytes upon PKA inhibition with H-89**

| | TgAFA-PLN + H89 | TgPLN + H89 | *P* |
|---|---|---|---|
| **N** | 7 hearts (77 cells) | 7 hearts (70 cells) | |
| **amplitude [ΔF]** | 0.50 ± 0.04 | 0.49 ± 0.03 | 0.68 |
| **vel increase [ΔF $s^{-1}$]** | 31 ± 3 | 35 ± 3 | 0.38 |
| **vel decrease [ΔF $s^{-1}$]** | 2.2 ± 0.2 | 2.2 ± 0.3 | 0.99 |

amplitude, peak height of the $Ca^{2+}$ transient; ΔF, change of fluorescence (340/380nm); vel increase (decrease), velocity of transient increase (decrease); *P* values by unpaired Student's *t* test.

## Supplementary Table S6

**Table S6: Sarcomere function in isolated myocytes**

| **baseline** | PLN-KO | TgAFA-PLN | *P* vs. PLN-KO | TgPLN | *P* vs. PLN-KO | *P* vs. TgAFA-PLN |
|---|---|---|---|---|---|---|
| **N** | 16 | 9 | | 10 | | |
| **max sarc length [µm]** | 1.78 ± 0.02 | 1.76 ± 0.02 | 0.67 | 1.76 ± 0.01 | 0.69 | 0.99 |
| **amplitude [nm]** | 145 ± 14 | 151 ± 22 | 0.96 | 115 ± 12 | 0.36 | 0.32 |
| **vel contraction [µm $s^{-1}$]** | 4.0 ± 0.7 | 3.6 ± 0.6 | 0.88 | 2.2 ± 0.3 | 0.10 | 0.33 |
| **vel relaxation [µm $s^{-1}$]** | 1.14 ± 0.13 | 1.05 ± 0.14 | 0.88 | 0.68 ± 0.10 | **0.04** | 0.19 |

| **$10^{-7}$ M isoprenalin** | PLN-KO | TgAFA-PLN | *P* vs. PLN-KO | TgPLN | *P* vs. PLN-KO | P vs. TgAFA-PLN |
|---|---|---|---|---|---|---|
| **N** | 16 | 9 | | 10 | | |
| **amplitude [nm]** | 160 ± 13 | 161 ± 14 | 0.99 | 152 ± 15 | 0.92 | 0.92 |
| **vel contraction [µm $s^{-1}$]** | 4.5 ± 0.5 | 4.9 ± 0.7 | 0.88 | 4.0 ± 0.6 | 0.79 | 0.58 |
| **vel relaxation [µm $s^{-1}$]** | 1.59 ± 0.20 | 1.30 ± 0.16 | 0.55 | 1.36 ± 0.20 | 0.68 | 0.98 |

N, number of hearts; max sarc length, sarcomere length of resting myocytes; vel contraction / relaxation, speed of sarcomere contraction / relaxation; *P* values by one-way ANOVA followed by Tukey's multiple comparisons test.

Figure 1A

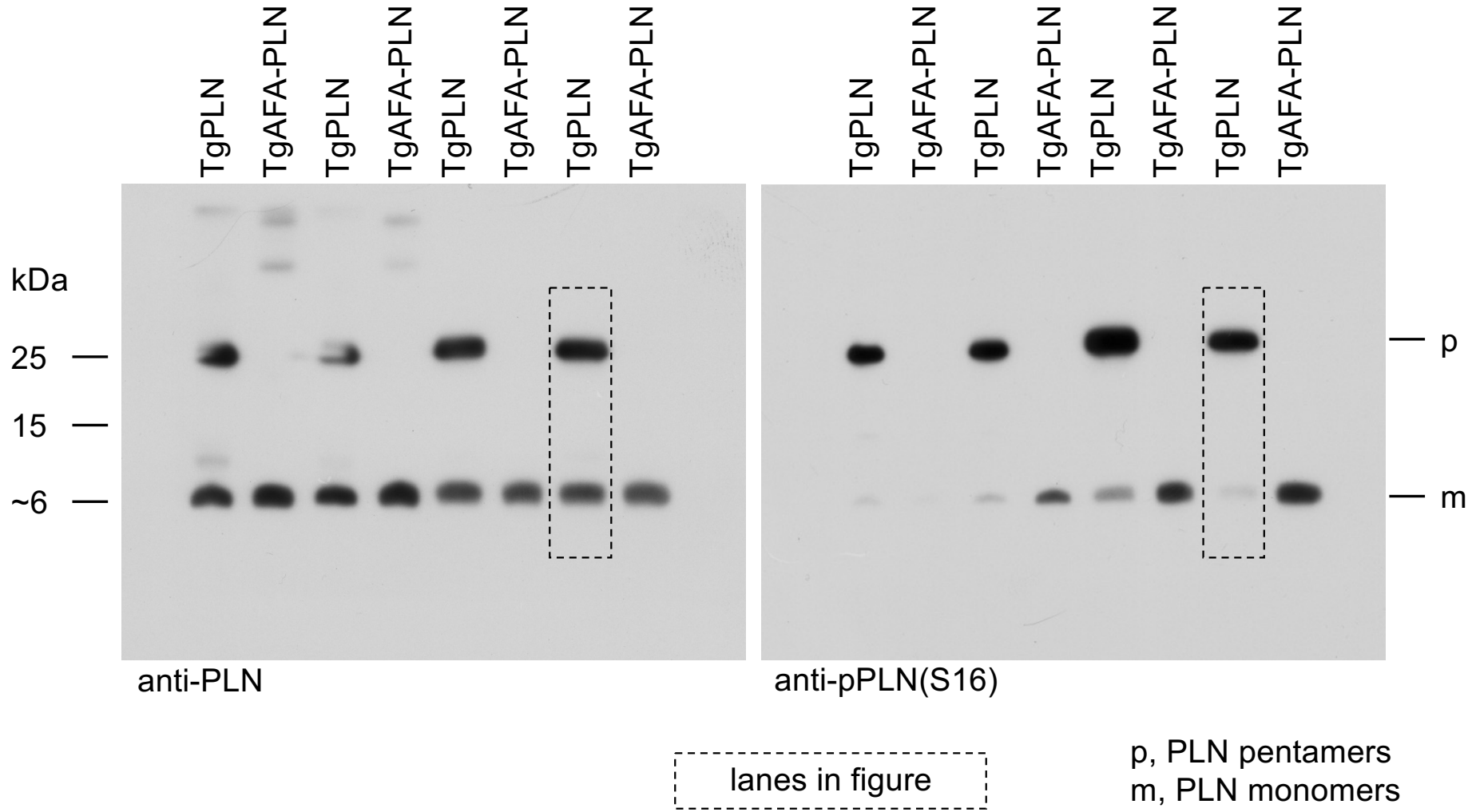
TgPLN
TgAFA-PLN
TgPLN
TgAFA-PLN
TgPLN
TgAFA-PLN
TgPLN
TgAFA-PLN
TgPLN
TgAFA-PLN
TgPLN
TgAFA-PLN
TgPLN
TgAFA-PLN
TgPLN
TgAFA-PLN
kDa
25
15
~6
p
m
anti-PLN
anti-pPLN(S16)
lanes in figure
p, PLN pentamers
m, PLN monomers

Figure 1B

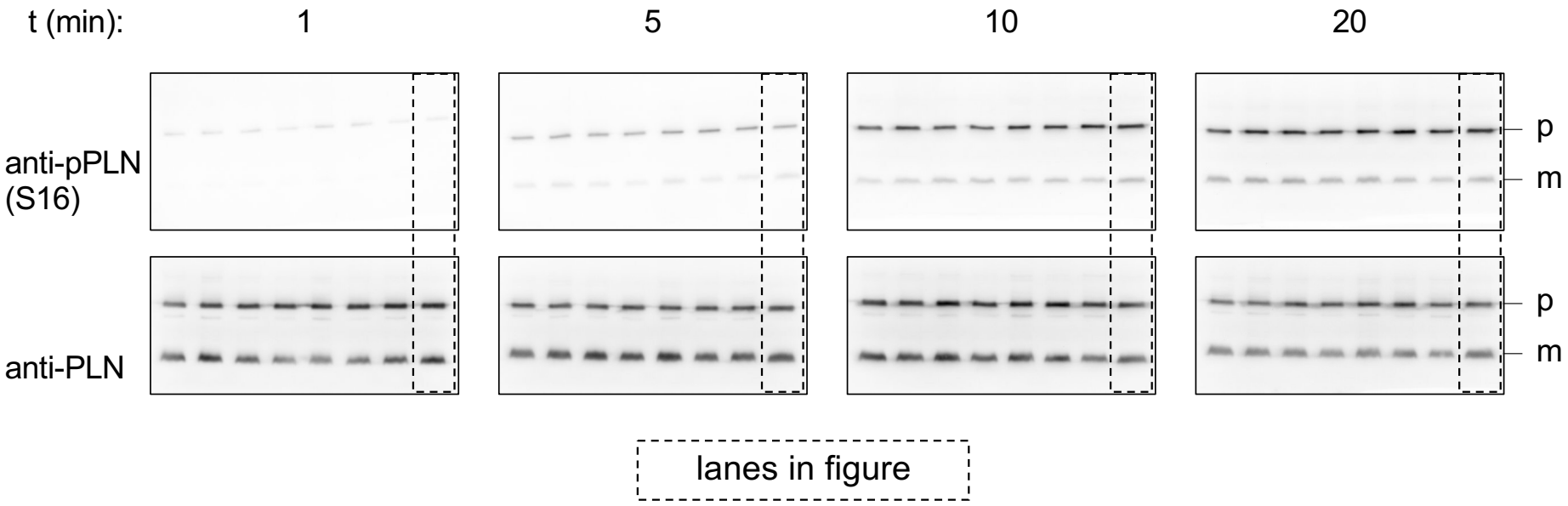


p, PLN pentamers (~25 kDa); m, PLN monomers (~6 kDa)

Figure 1D

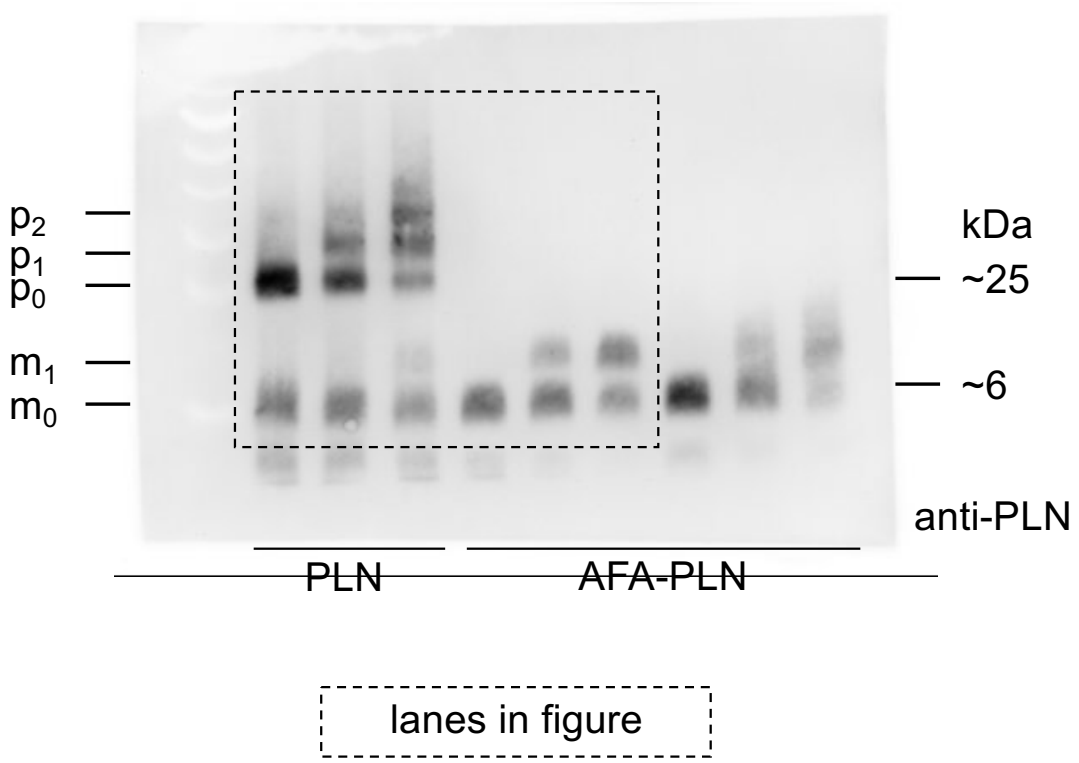

Figure 2A

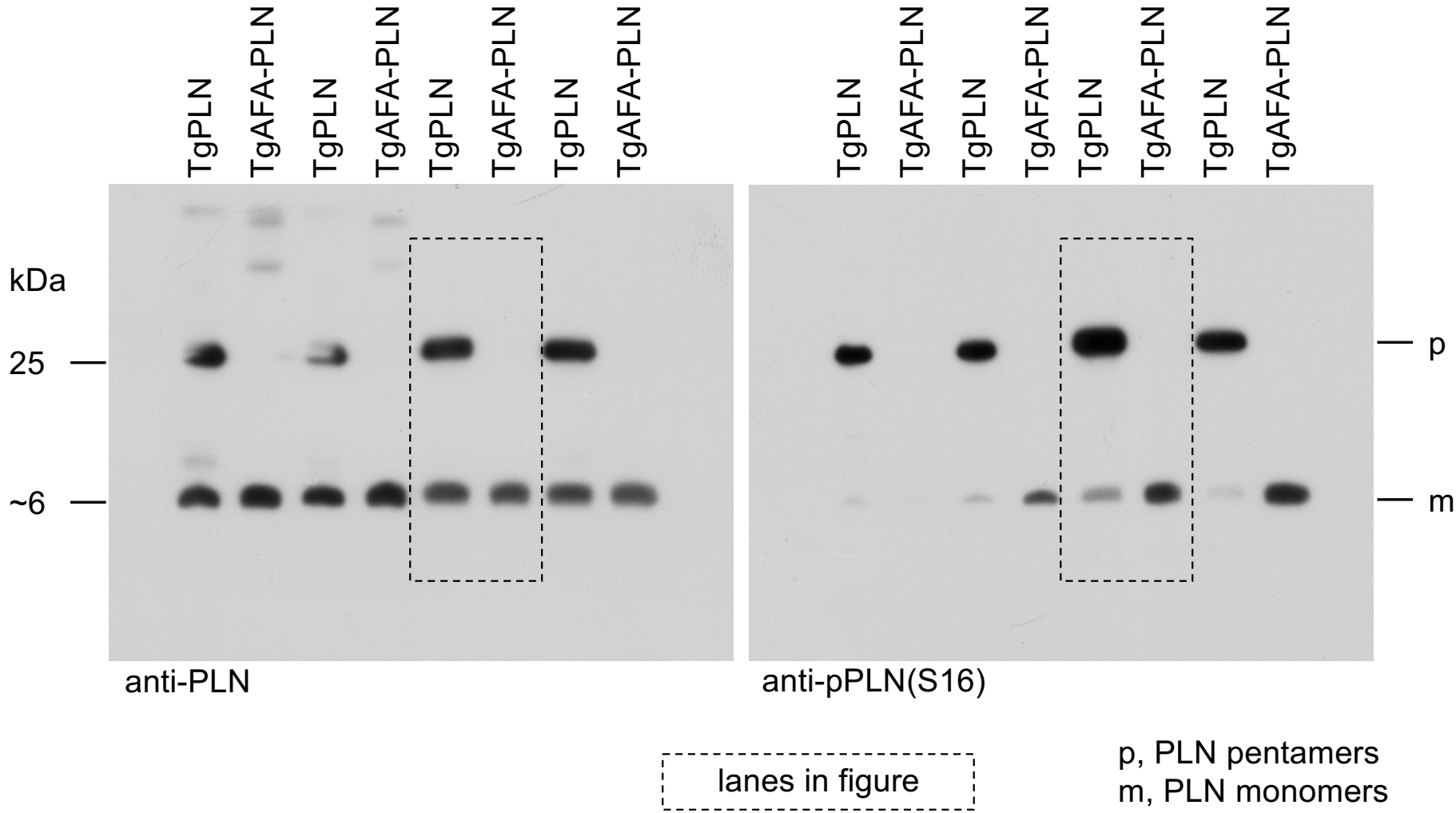
TgPLN
TgAFA-PLN
TgPLN
TgAFA-PLN
TgPLN
TgAFA-PLN
TgPLN
TgAFA-PLN
TgPLN
TgAFA-PLN
TgPLN
TgAFA-PLN
TgPLN
TgAFA-PLN
TgPLN
TgAFA-PLN
kDa
25
~6
p
m
anti-PLN
anti-pPLN(S16)
lanes in figure
p, PLN pentamers
m, PLN monomers

Figure 2B

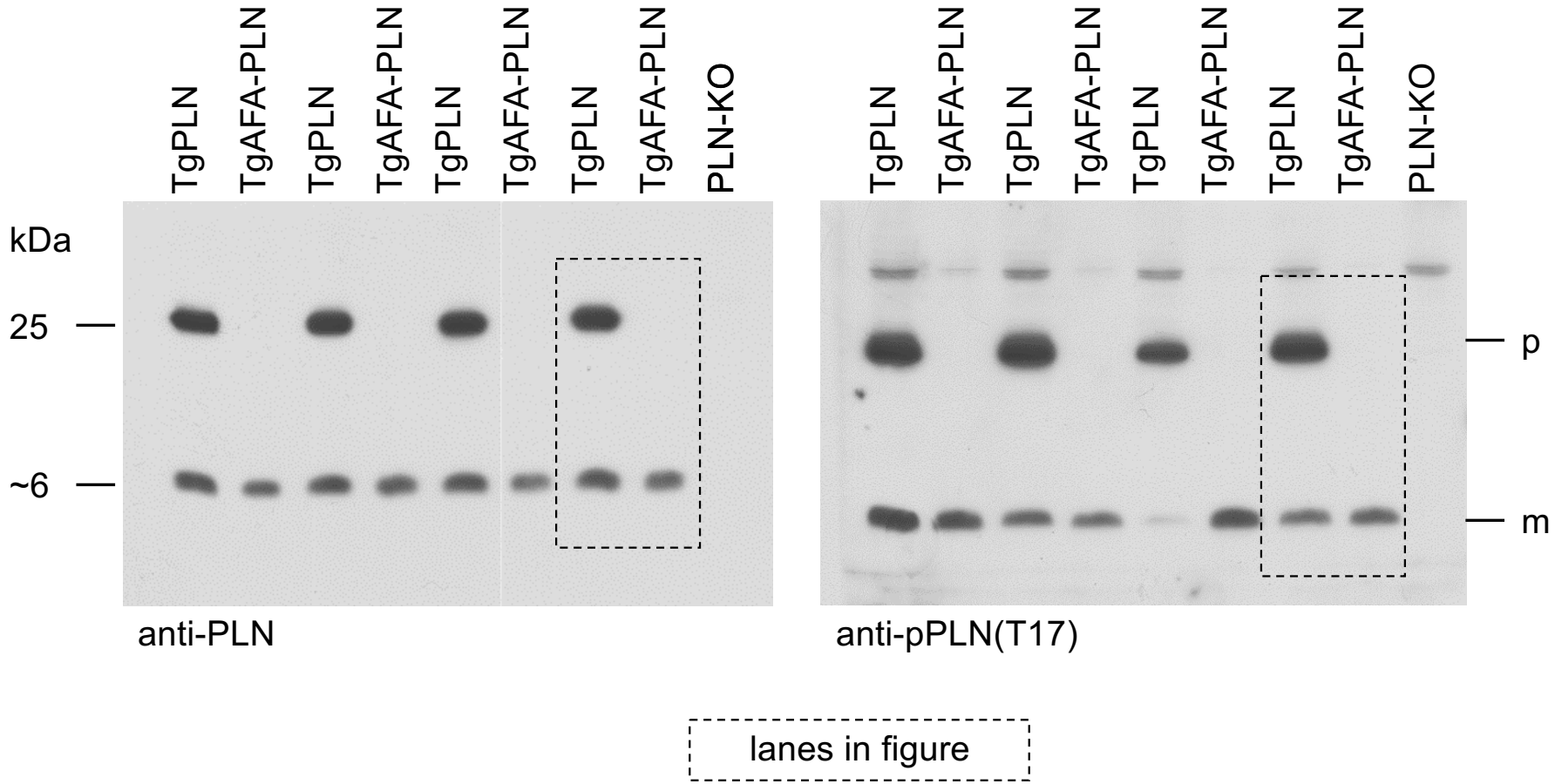
TgPLN
TgAFA-PLN
TgPLN
TgAFA-PLN
TgPLN
TgAFA-PLN
TgPLN
TgAFA-PLN
PLN-KO
kDa
25
~6
anti-PLN
TgPLN
TgAFA-PLN
TgPLN
TgAFA-PLN
TgPLN
TgAFA-PLN
TgPLN
TgAFA-PLN
PLN-KO
p
m
anti-pPLN(T17)
lanes in figure

Figure 2C

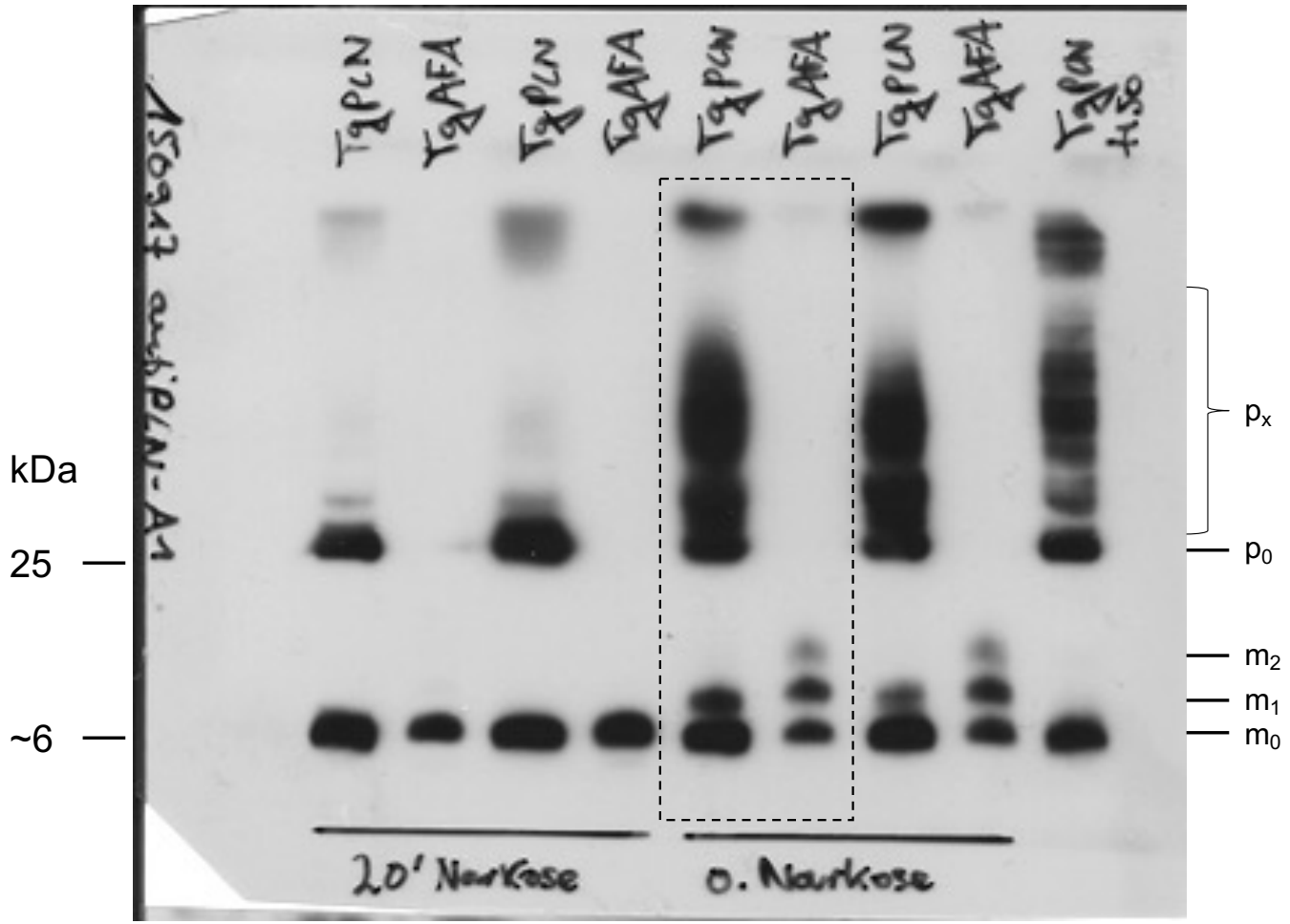


lanes in figure

$m_0/p_0$, unphosphorylated PLN monomers/pentamers; $m_x/p_x$ (x=1, 2, …), PLN monomers/pentamers carrying x phosphate residues; anti-PLN

Figure 2D

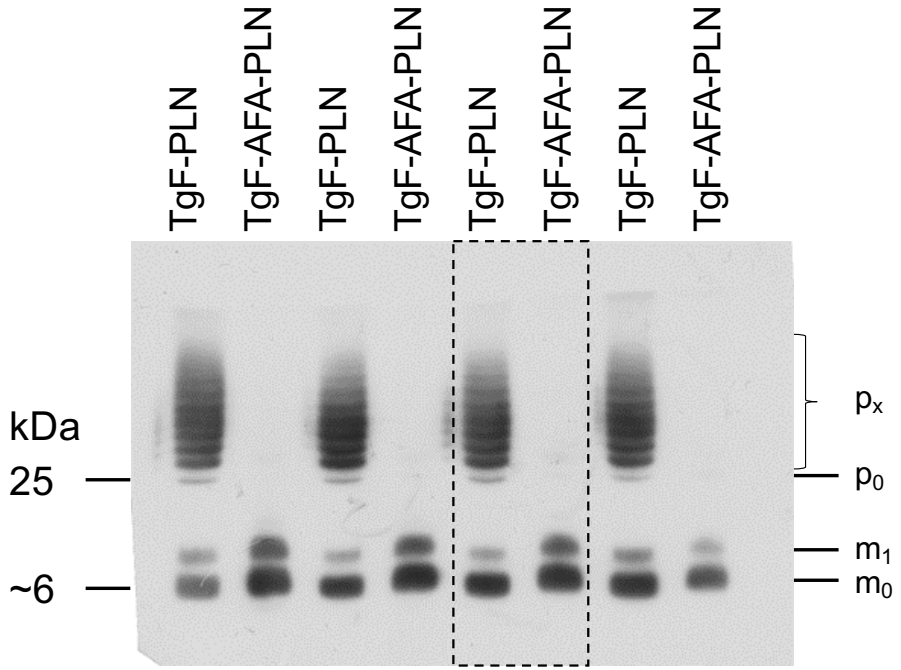


$m_0/p_0$, unphosphorylated PLN monomers/pentamers; $m_x/p_x$ (x=1, 2, …), PLN monomers/pentamers carrying x phosphate residues; anti-FLAG

lanes in figure

Figure 3A

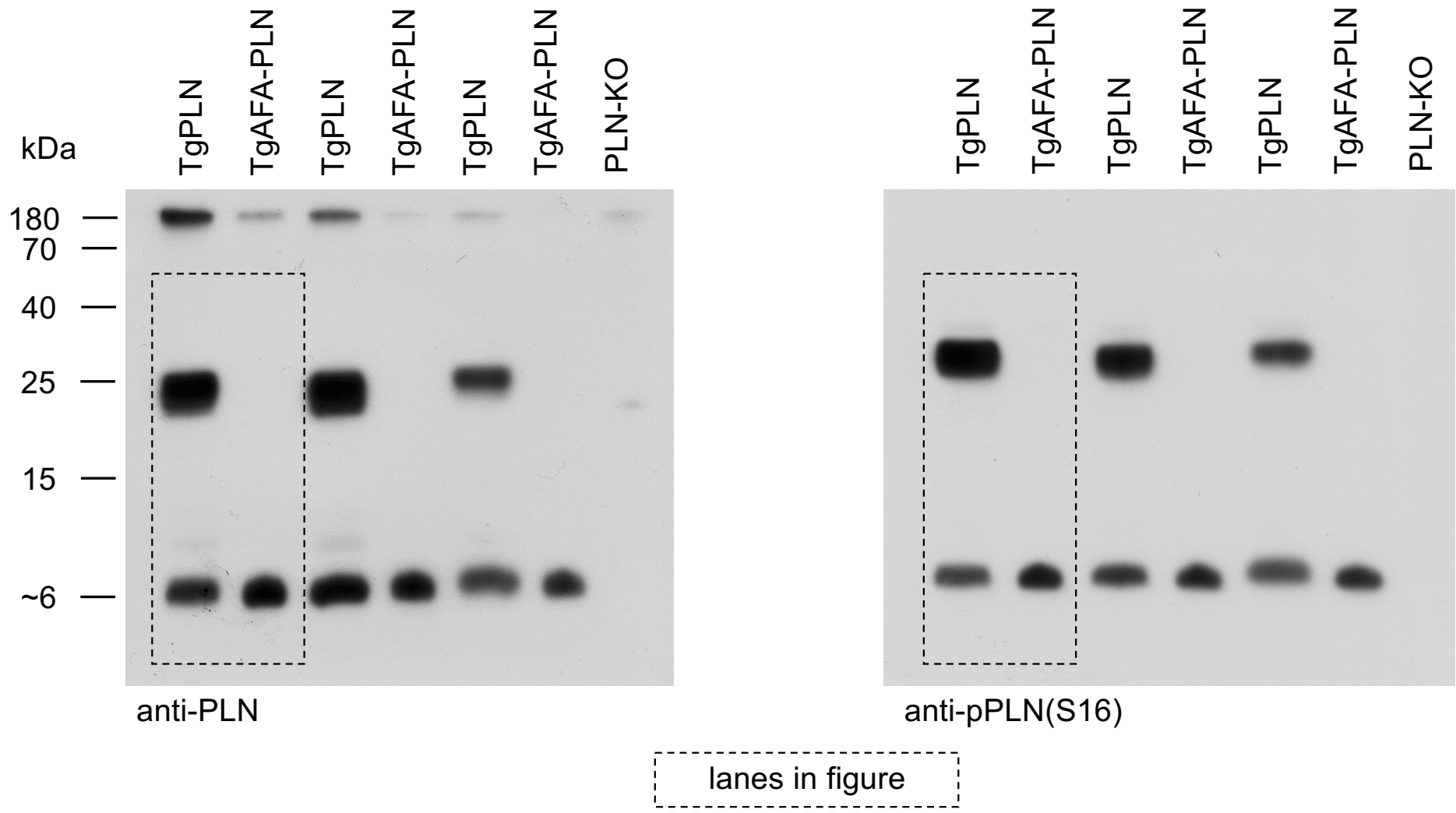
kDa
TgPLN
TgAFA-PLN
TgPLN
TgAFA-PLN
TgPLN
TgAFA-PLN
PLN-KO
180
70
40
25
15
~6
anti-PLN
TgPLN
TgAFA-PLN
TgPLN
TgAFA-PLN
TgPLN
TgAFA-PLN
PLN-KO
anti-pPLN(S16)
lanes in figure

Figure 3C

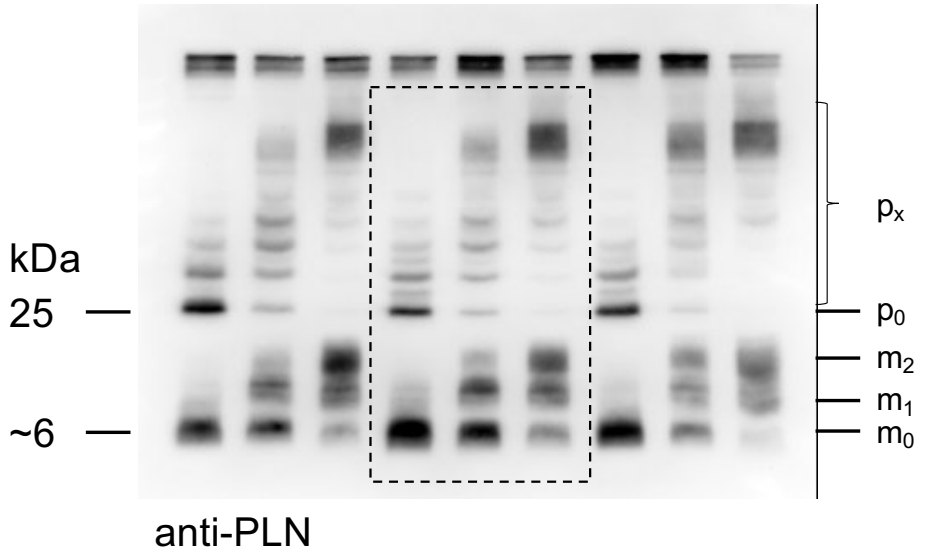


$m_0/p_0$, unphosphorylated PLN monomers/pentamers;
$m_x/p_x$ (x=1, 2, …), PLN monomers/pentamers carrying x phosphate residues

lanes in figure

Figure S1

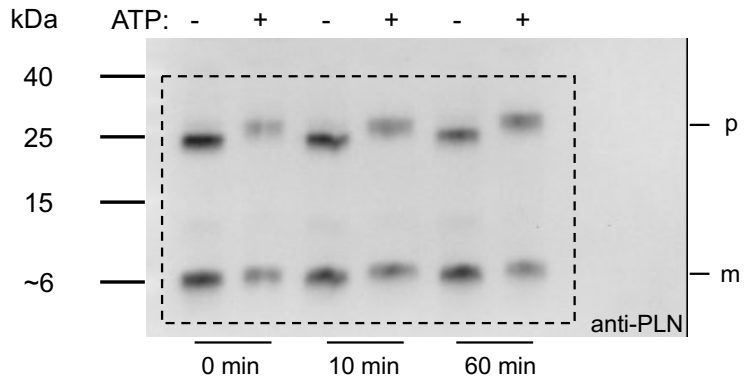


p, PLN pentamers; m, PLN monomers

Figure S2

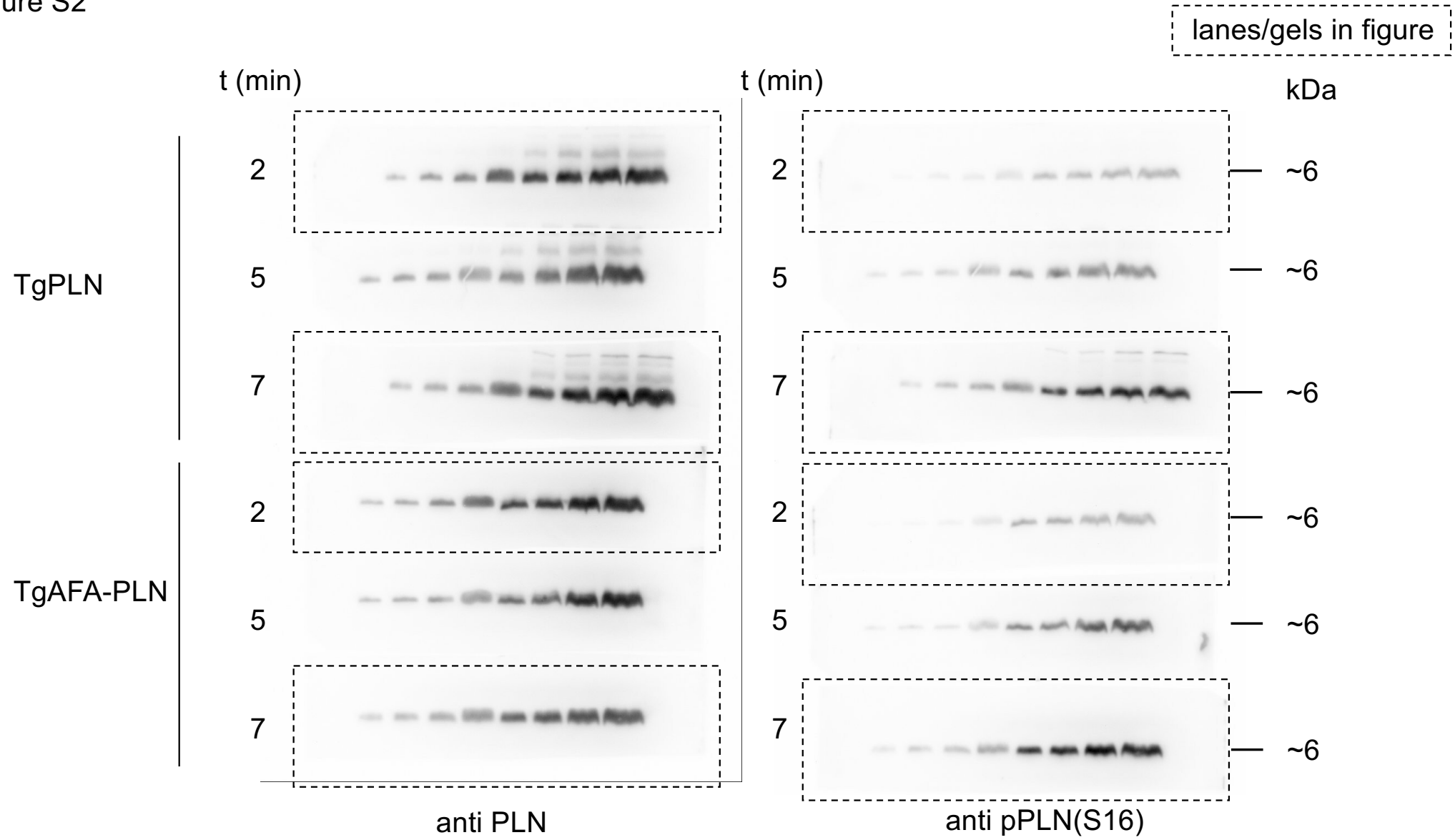
lanes/gels in figure
t (min)
t (min)
kDa
TgPLN
TgAFA-PLN
2
5
7
2
5
7
2
5
7
2
5
7
~6
~6
~6
~6
~6
~6
anti PLN
anti pPLN(S16)

Figure S3

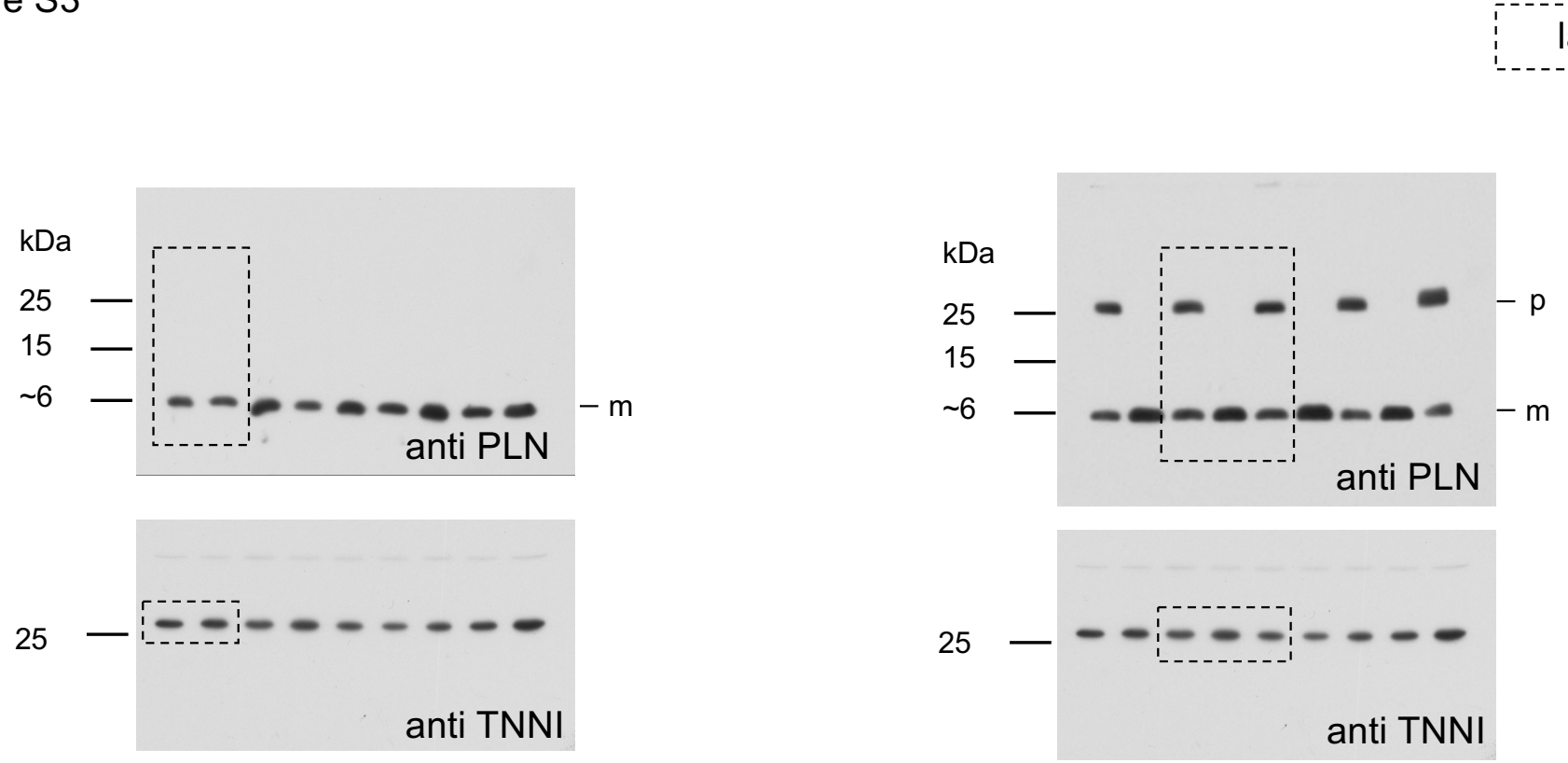


p, PLN pentamers (~25 kDa); m, PLN monomers (~6 kDa)

Figure S6

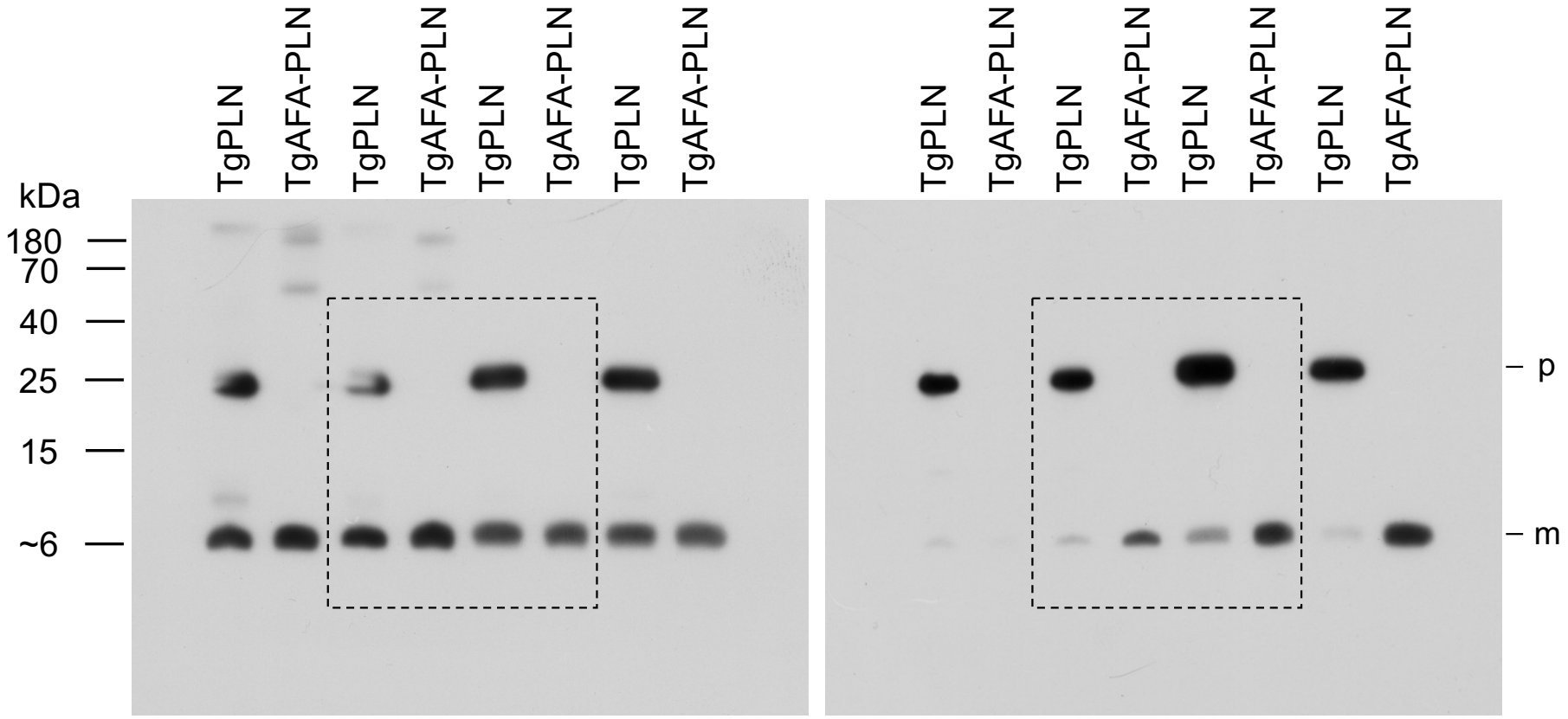


p, PLN pentamers (~25 kDa); m, PLN monomers (~6 kDa)

Figure S7

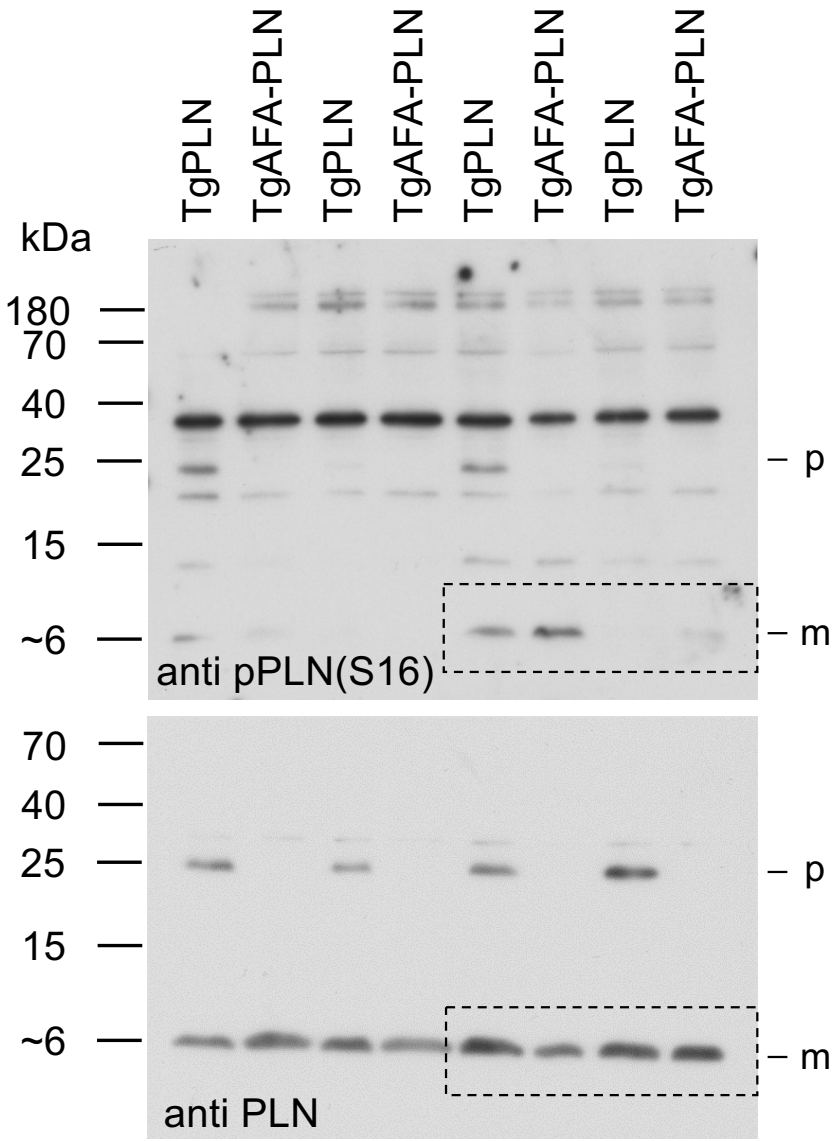


p, PLN pentamers (~25 kDa);
m, PLN monomers (~6 kDa)

lanes in figure

Figure S8A

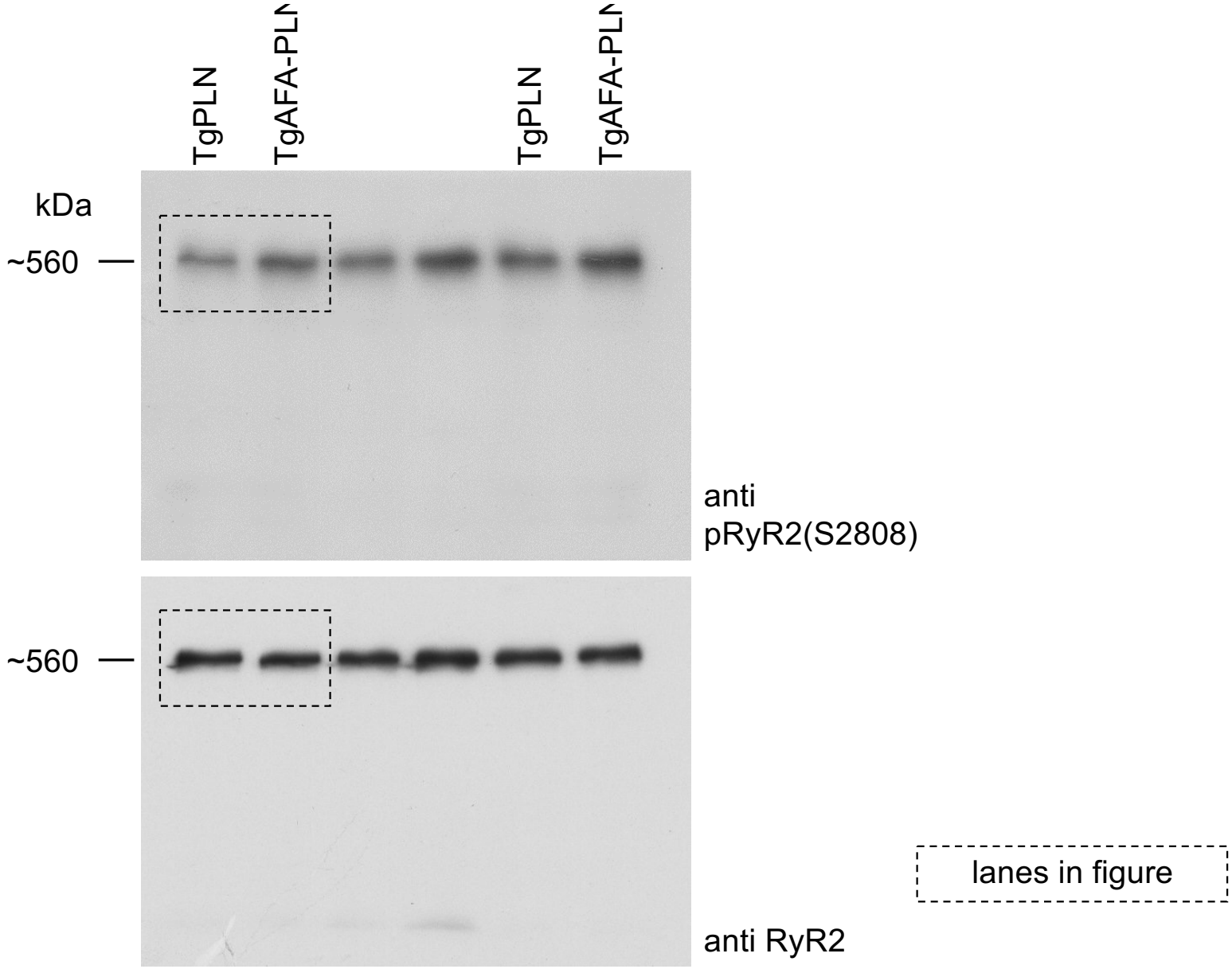
TgPLN
TgAFA-PLN
TgPLN
TgAFA-PLN
kDa
~560
anti
pRyR2(S2808)
~560
anti RyR2
lanes in figure

Figure S8B

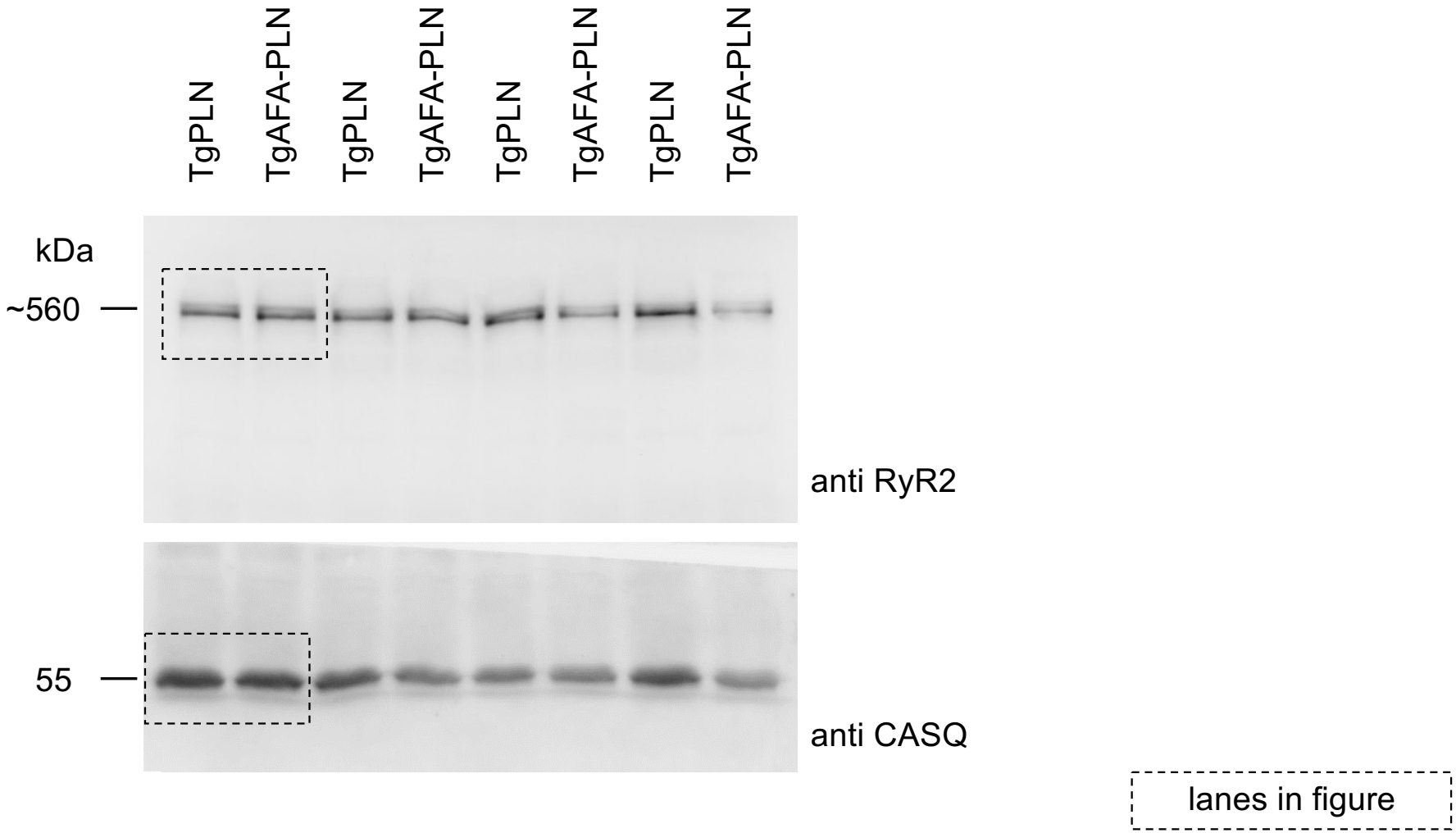
TgPLN
TgAFA-PLN
TgPLN
TgAFA-PLN
TgPLN
TgAFA-PLN
TgPLN
TgAFA-PLN
kDa
~560
anti RyR2
55
anti CASQ
lanes in figure

Figure S8C

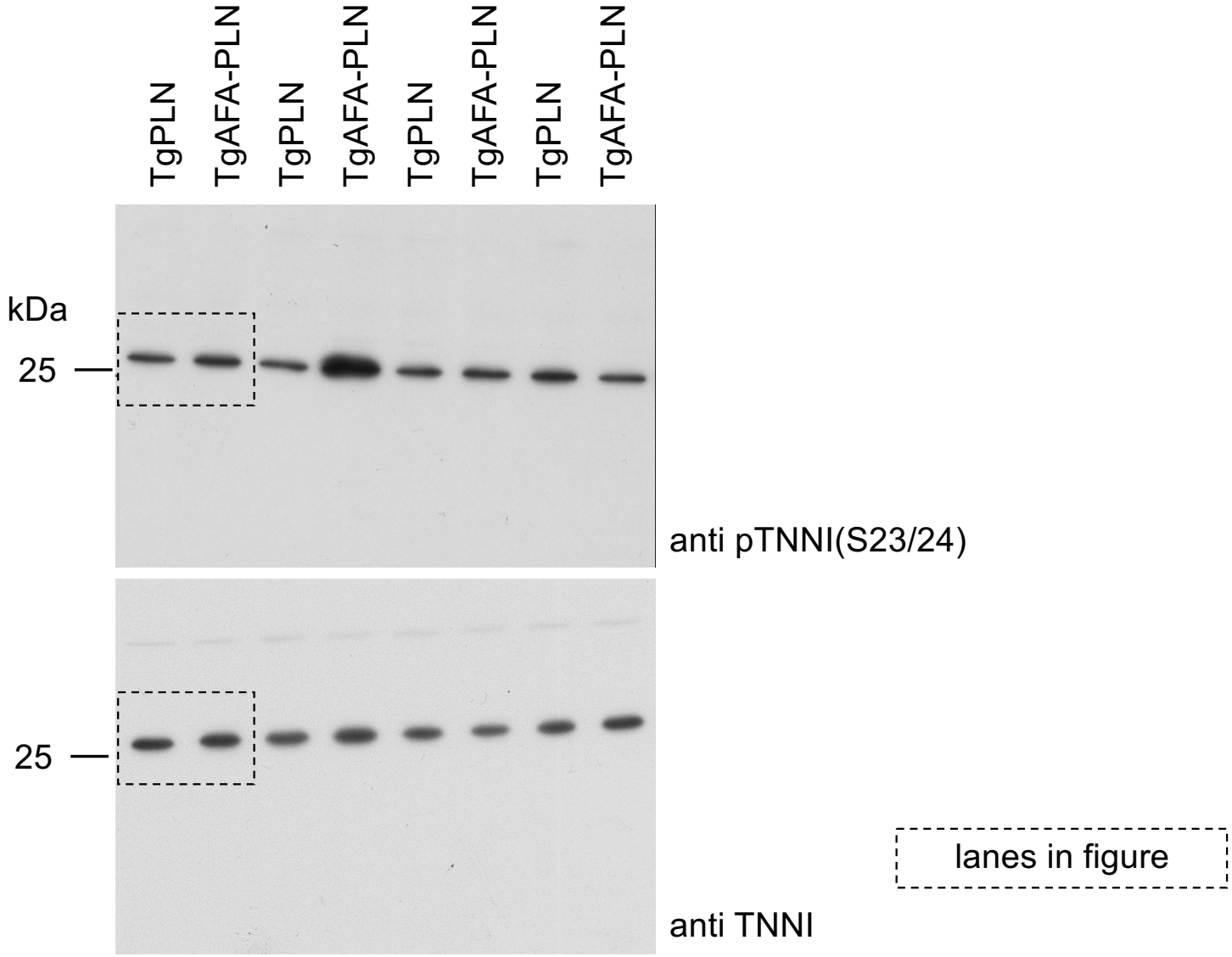
TgPLN
TgAFA-PLN
TgPLN
TgAFA-PLN
TgPLN
TgAFA-PLN
TgPLN
TgAFA-PLN
kDa
25
anti pTNNI(S23/24)
25
anti TNNI
lanes in figure

Figure S8D

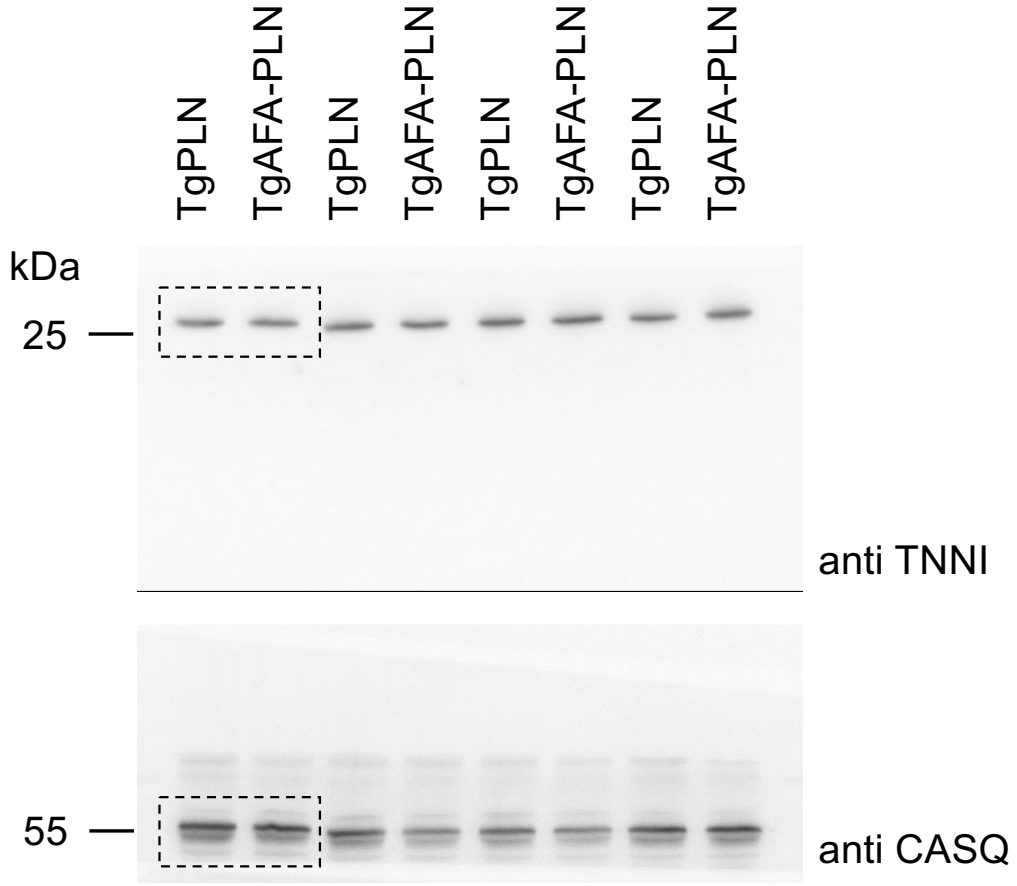
TgPLN
TgAFA-PLN
TgPLN
TgAFA-PLN
TgPLN
TgAFA-PLN
TgPLN
TgAFA-PLN
kDa
25
anti TNNI
55
anti CASQ
lanes in figure

Figure S8 E,F,G

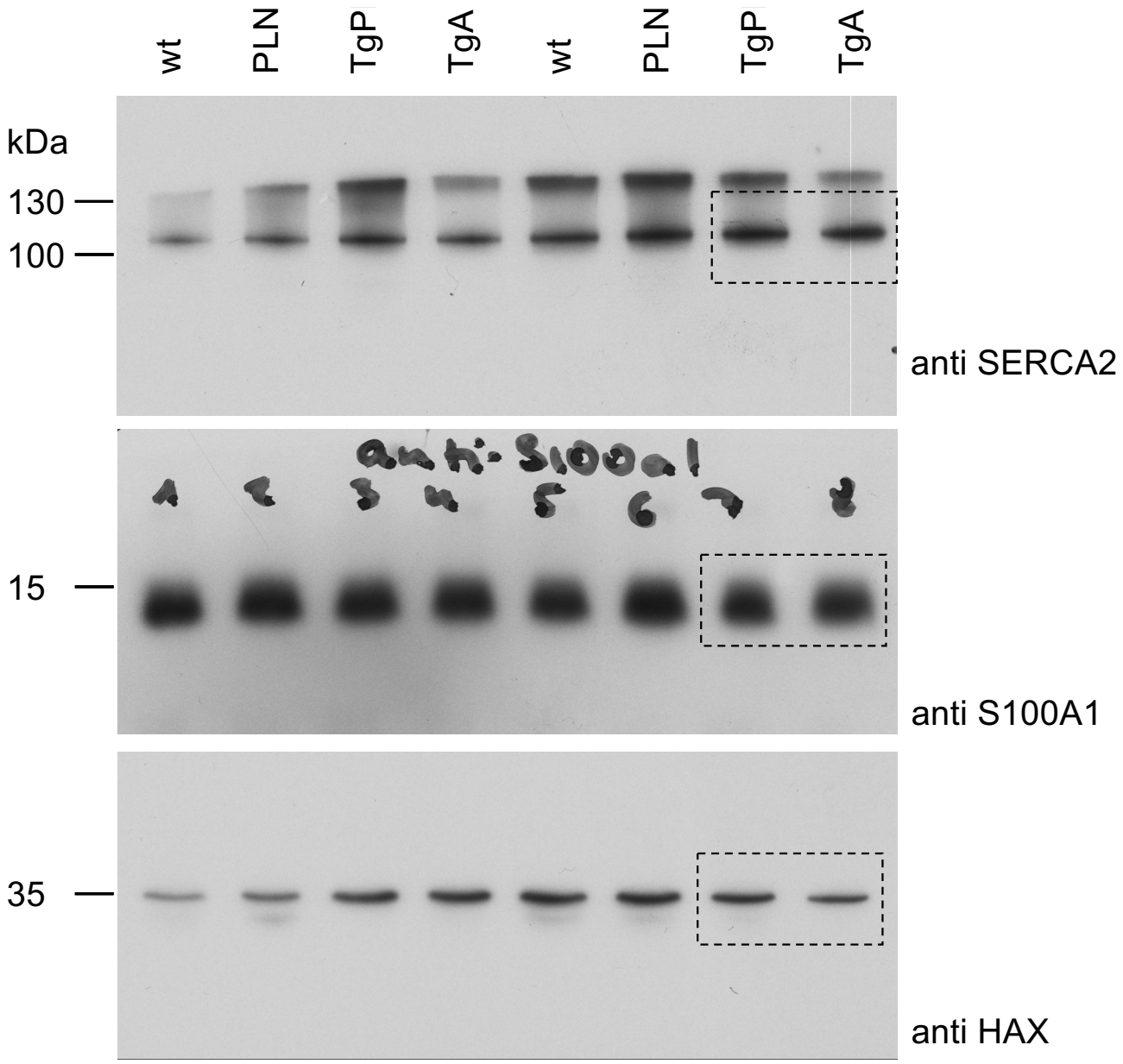

Figure S10

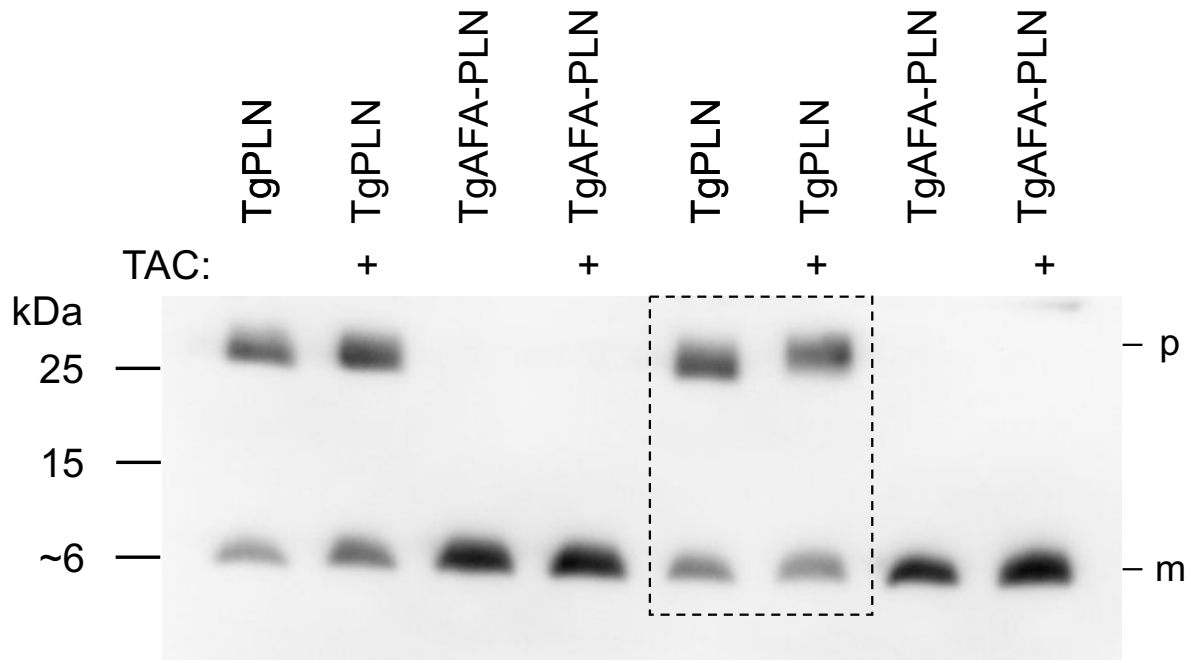


lanes in figure

p, PLN pentamers (~25 kDa); m, PLN monomers (~6 kDa)

Figure S11

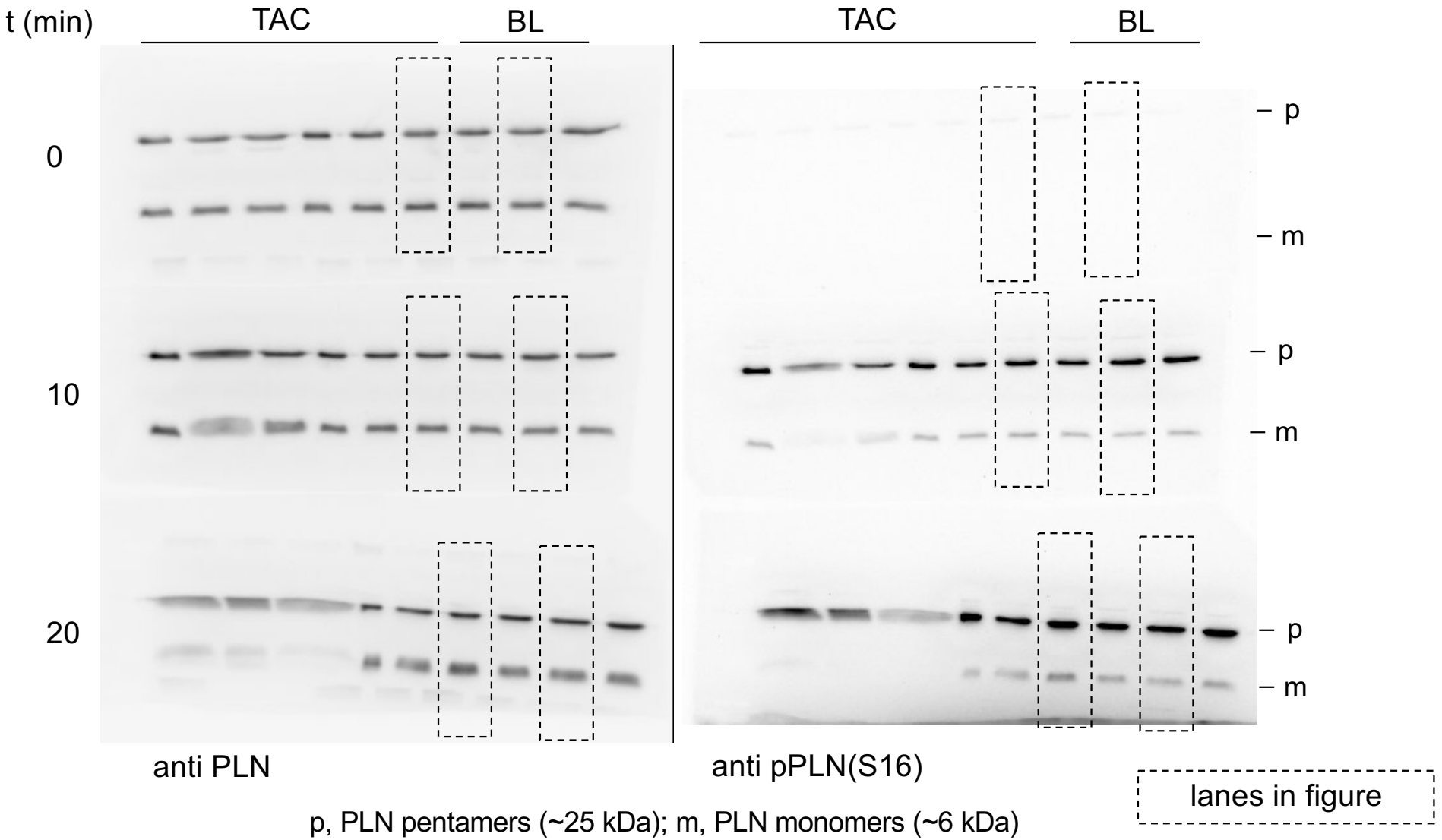


p, PLN pentamers (~25 kDa); m, PLN monomers (~6 kDa)

Figure S12 A

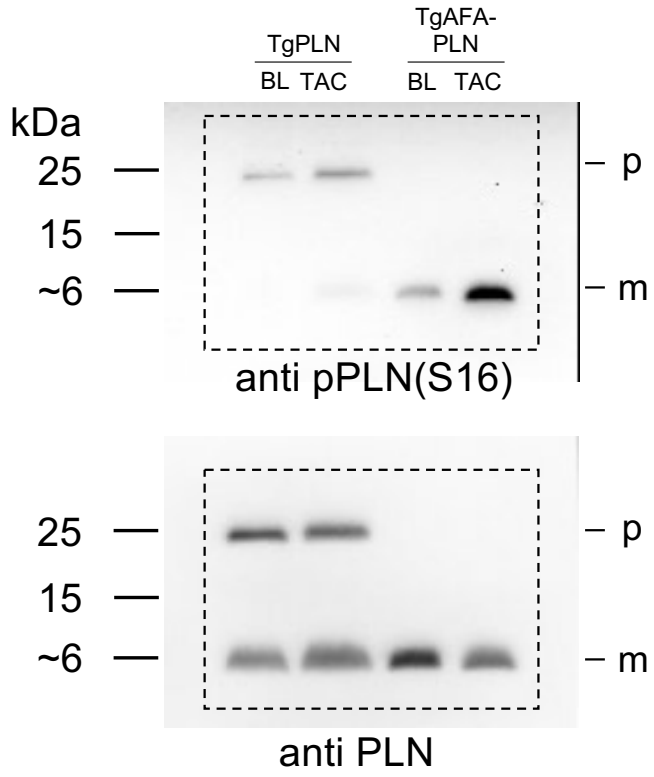


p, PLN pentamers (~25 kDa); m, PLN monomers (~6 kDa)

lanes in figure

Figure S12 B

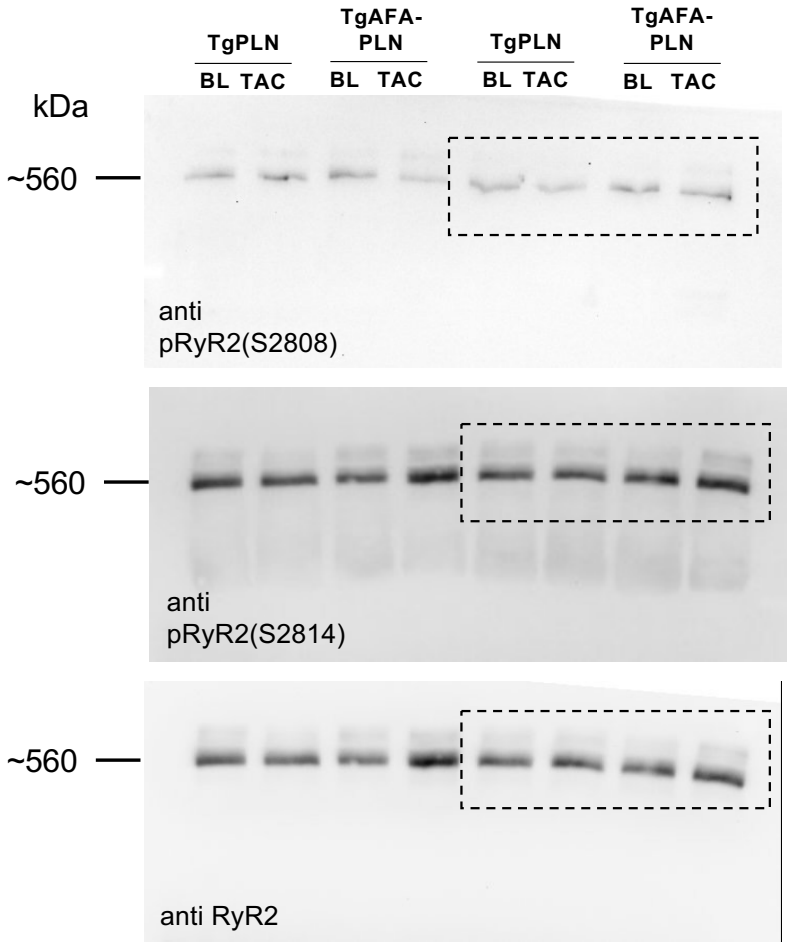


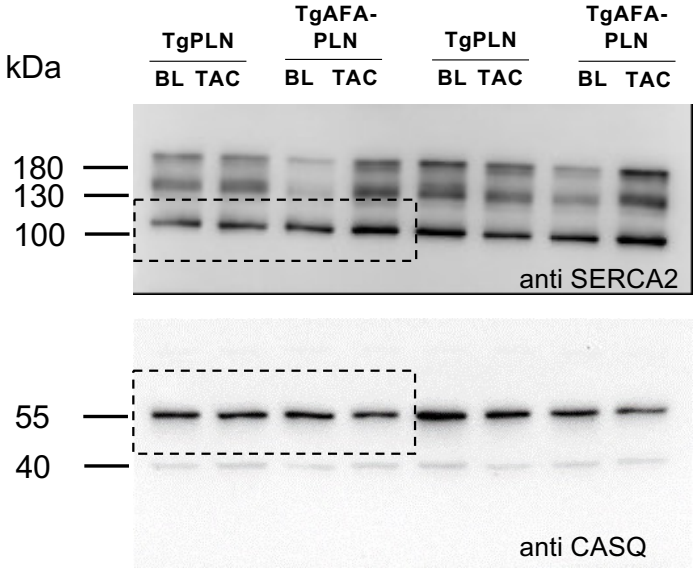


lanes in figure

Figure S13

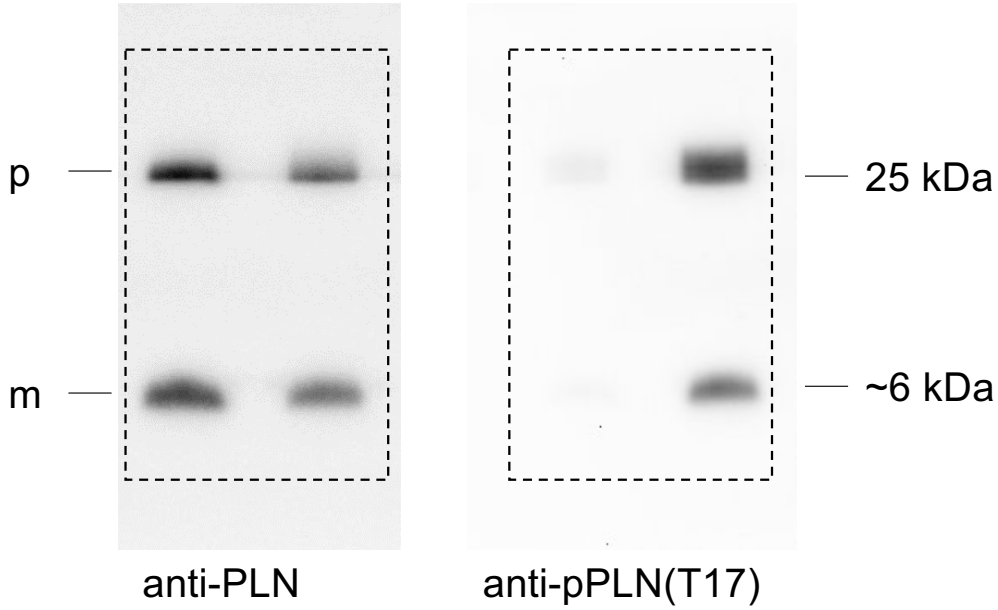


p, PLN pentamers (~25 kDa); m, PLN monomers (~6 kDa)

Figure S14

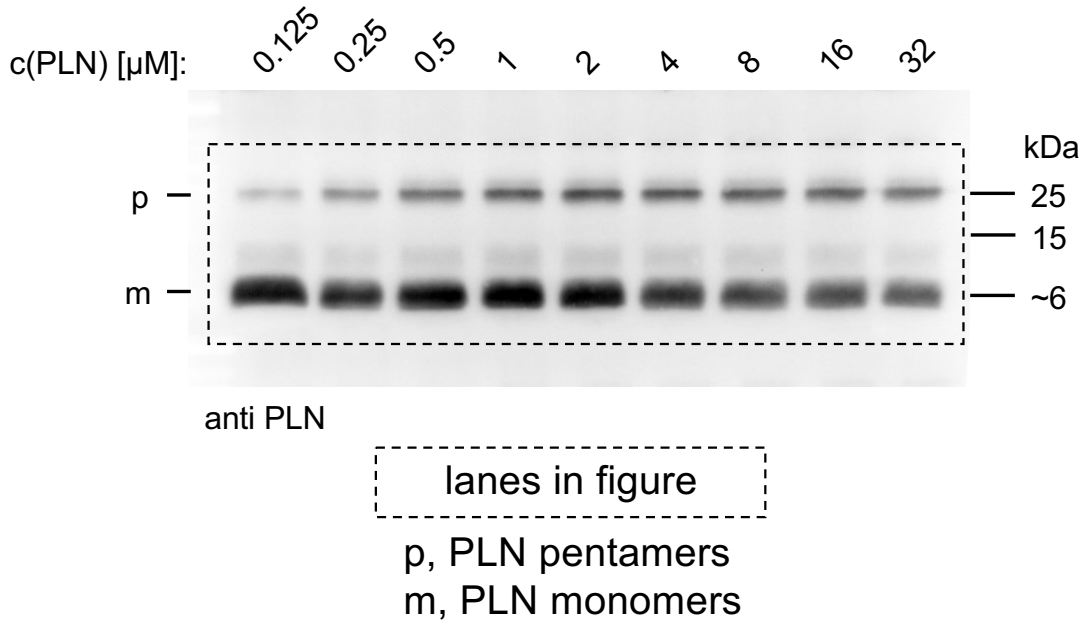
c(PLN) [µM]:
0.125
0.25
0.5
1
2
4
8
16
32
kDa
p
m
25
15
~6
anti PLN
lanes in figure
p, PLN pentamers
m, PLN monomers